

Dear Editor,

We are thankful for this round of constructive and highly relevant reviews that helped us to improve the manuscript significantly. We hereby resubmit the manuscript for your consideration. Please find below the answers to each raised point by the referees and how the changes were implemented. The main changes in the manuscript can be summarized as follow:

- We have performed additional sensitivity tests for the geometry of the ridges in the model. The result is included in the supplementary, this include an additional figure. The main outcome of the additional tests is also presented in the main text.
- We have changed the paper structure to show a clear separation between results and discussion.
- The section where the model results is presented (5.1) includes now a paragraph that develops on the assumption of coupling between deep crustal and near surface deformation.
- We explain in the introduction the use of the terminology active vs. inactive pockmarks and refer to the presence or not of acoustic flares when possible.
- The discussion has been significantly extended: we developed further the analysis of modelled tectonic stress in the context of the total state of stress in the region; and we present a more substantial description of how we envision the evolution of present day and past seepage activity along the VR (including the mechanical relation between gas chimneys and faults). We close the discussion by placing our study in a context of global implications.
- All the specific comments have been addressed.
- Several figures were edited to support implemented changes. A new inset was included in former figure 3. A new figure is included in the result section to illustrate the origin of the tensile zone that extends towards the eastern Vestnesa Ridge. The figure numbers was updated accordingly. A figure for illustrating the model geometry was re-inserted in the appendix (we believe we lost that figure in the previous submission).
- Abstract, Introduction and conclusion sections were edited accordingly.

Sincerely,

Andreia Plaza-Faverola and Marie Keiding

Referee #1

In this contribution the authors are trying to bring together tectonic modeling (stress/strain) and observations on fluid seepage at Vestensa, off Svalbard. Their model suggests a region of tensile stresses that mostly coincides with a region of actively degassing pockmarks on the Vestnesa Ridge, juxtaposed to zones of strike-slip stress and inactive pockmarks.

I am reviewing this contribution after a first initial set of reviews by different reviewers was completed. I am judging my response on (a) the scientific material presented in the revised manuscript and (b) the earlier comments made by one reviewer on the applicability of the model used.

I find the approach presented in this manuscript intriguing, results rather interesting, but remain skeptical on the conclusions drawn. The paper needs some modifications, especially more discussions and at least one other set of tests if the zone of tensile stress is indeed robust in its location by modifying plate boundary geometries (which can be drawn differently than what authors show).

A few general remarks that I think would help in getting this paper published:

(a) Pockmarks on the southern drift. The authors show faults mapped south of the MTF, where seismic and bathymetric data show abundant chains of pockmarks. Those pockmarks are inactive in the terminology of the authors (i.e. inactive= no degassing). I suggest the authors augment their discussion on how to explain those southern pockmark chains as well. The orientation of principle stresses is strikingly different south and north of the MTF, relative to mapped fault-orientations (parallel, perpendicular) and earthquake focal mechanisms. Why is this not important as well?

Answer: thanks for pointing out this. The original focus of the paper was entirely on the Vestnesa Ridge seepage system (we wanted to test the hypothesis put forward in Plaza-Faverola et al., 2015). Also Vestnesa Ridge is much better studied than any other sedimentary ridge in the area. Having said that, we reckon that the correlation of these areas with the modeled stress fields makes sense.

Changes: We have included the location of these pockmarks in the discussion. Projection of pockmarks south of the MTF and right north of it where acoustic flares have not been documented as for the eastern Vestnesa ridge (i.e., Waghorn et al., 2018; Johnson et al., 2015) and discuss the spatial correlation of these features with the predicted stress field. We do emphasize that the features are less well investigated and a poorer control exist on the activity of this system. Ongoing studies by colleagues will provide more information about the structural setting in these regions.

(b) Why only use degassing as sign of “activity”? Very recent heat-flow surveying (>100 measurements) taken across the pockmarks show that pockmarks may be still “active” even without gas discharge, as they can show a strong and localized heat-flow anomaly to the pockmark depressions themselves (and that occurs north and south of the MTF and the zone of tensile stress regime). The authors are aware of this study and data as well as preliminary results from the heat-flow study are available through the cruise report of expedition MSM57 and can be downloaded from the University of Bremen website.

Answer: We are aware of this recent heat flow study, yes. This is of course a relevant point in the sense that the terminology used is crucial. Despite anomalous heatflow measured nearby fault planes and pockmarks in the region (also Crane et al., in the late 90s show this), there is sufficient bubbling of gas only at discrete sites. The University of Tromsø goes to the region sometime 2 times a year, and vertical acoustical anomalies in the multibeam and echo-sounder profiles (so call acoustic gas flares) are observed systematically on the few pockmarks on the astern Vestnesa Ridge segment. The pockmarks at the Svyatogor ridge and north of the MTF have been surveyed also several years (despite having received much less attention so far). Here, acoustic flares have also not been observed. The terminology we use then uses “active” for sites where seepage is enough to cause a visible anomaly in water acoustic data. The inactive adjective does not rule out advection of fluids toward the near-surface nor degassing to a certain but minor degree compared to the “active” sites.

Changes: we have clarified this through the text and figures. We also use the direct formulation of “documented acoustic flares” when possible.

- (c) Degassing could be completely unrelated to the deep-rooted stresses – microbial activity rates are changing; there is coupling between ocean phenomena and the sediment with free gas phases and gas hydrates (e.g. seen in tidal modulated gas fluxes or decadal oscillations). I think, using degassing alone is “too short” an argument to investigate the relationship between stress and the fluid flow regimes.

Answer and changes: We have provide additional background on the fluid flow and seepage system along the ridge to make clear why current changes in sea-level and temperature would not be sufficient to explain solely the dynamics in this deep marine system. Yes, microbial methane generation is always a contribution to the seepage system. Along the Vestensa Ridge thermogenic gas (methane, ethane, propane, butane, etc) have been sampled in head space samples from gravity cores as well as from water column and gas hydrate samples (e.g., Smith et al., 2014). The fluid flow systems is well documented to be associated with faults that extend close to the seafloor; gas chimneys are indeed following the fault planes. Petroleum modeling suggest that a thermogenic gas source may have been charging the system since 2 Ma ago (Knies et al., 2018). In this paper we rely on all these studies to assume that the advection of thermogenic/warmer fluids into the near-surface is a key player in gas hydrates and seepage dynamic in the region. Whether there is in addition seepage controlled by local microbial methane generation and to a small degree gas hydrate dissociation, is not so critical for this study. Regardless the source of the gas the behavior of faults can be modulating gas release.

- (d) Sediment drift bodies such as the Vestensa Ridge are heavily dynamic and evolve quickly. Topography is steep across the ridge and vertical stresses thus change fast. While the authors do say and have indicated in the revised version of their manuscript that they do not reject other causes (and associated stresses) of the difference in vent activity, but I find the outcome or limitation of discussion only on the zone of tensile stress rather weak overall, given this very dynamic and regionally fast-changing zone of study.

Answer and changes: we have now significantly extended the discussion to present clearer why the proposed tectonic explanation is so relevant for the study area and we provide summary of observations (large number of cross disciplinary studies) that points toward a regional tectonic mechanism.

- (e) The geometry of the plate boundaries, especially the MTF, seems to be fixed in all the discussion, but I could easily draw the MTF at a different angle (e.g. rotated by 5 degrees) by just looking at the bathymetry. Would this not affect the zone of tensile stress regime? The authors did look at parameter variations and assess effects in the actual zones of stresses, but they never changed the geometry. Maybe test quickly, if this is important or not?

Answer and changes: Thanks for this suggestion. We carried out additional tests of the geometry by rotating the MTF as well as the MR and KR. The geometry does influence the shape or position of the tensile zone. However, the zone persists approximately in place. We have included results of diverse tests on geometry in the supplementary material. We also clarify, by including a new figure, how the tensile zone results due to the interaction between the spreading force from the Molloy and Knipovich ridges.

- (f) Coupling between crustal deformation and sediment load seems to have been assumed as 100%. Is that acceptable? Could those regimes be decoupled, i.e. the ridge-push is doing its own thing and sediment drape from contourites deposited during glacial/deglacial phases react to other forces?

Answer and changes: We agree that this is a crucial and exciting question related to the topic. Is there a full coupling between crustal deformation and near-surface deformation of quaternary sediments? We discuss our results assuming a certain degree of coupling, as pointed out by the referee. We argue the near-surface faults reflect coupling (we interpret them as tectonic faults). We added a paragraph in section 5.1 with arguments supporting the assumption of a certain degree of coupling. We also touch upon the implications of assuming the coupling for the current debate about activity across passive margins.

Overall, the manuscript has its contribution that is interesting and intriguing, fully worth of getting published at some point; but as of yet, it has too little result and discussion to be fully acceptable. After the initial revision, the authors modified and restated many points in their discussion and conclusion but need to go even further. I suggest a more diverse discussion taking some of my points above into account and possibly assess the “error” in the stress-regime mapping a step further.

Then, what are the larger implications of such process? Could you maybe name other regions where similar processes occur? What other studies would help assess this phenomenon further? Borehole stress measurements? Are there maybe wire-line image log (from resistivity) data from the old ODP boreholes to look at the borehole stress by mapping breakouts or fractures? Could you use the shear-wave splitting technique to look at the stress components by doing a polarization analysis of the first arrivals (e.g. Tonegawa et al., 2016)? Are those changing across Vestnesa and to the Svyatogor Ridge south of the MTF?

Answer: great suggestions here, thanks. We keep this in mind for further work on the topic. We have indeed on-going OBS experiments in the region. It would be interesting to further discuss the approach in the Tonegawa et al paper.

Changes: we added a paragraph on the discussion to place the outcome of the study into a global context, emphasizing other known seepage systems where a stress control can be applicable.

Tonegawa, T., Obana, K., Yamamoto, Y., Kodaira, S., Wang, K., Riedel, M., Kao, H., Spence, G.D., 2016. Fracture alignments in marine sediments off Vancouver Island from Ps splitting analysis, Bulletin of the Seismological Society of America, 10.1785/0120160090.

Referee #2

Dear Authors,

Understanding flow localisation patterns and location is a challenging enterprise. The submarine features leading to the expulsion of methane and other gases are widely reported, but currently the mechanisms remain still very unclear and discussed. In this context, this study tries to address a challenging point, constraining the flow localisation in Western Svalbard based on a analytical mechanical model of the complex lithospheric regional layout.

Although the model used seems to be correctly applied, the major simplifications and hypotheses the authors make in order to use it significantly limit the conclusion that can be drawn. This point was also discussed and criticised in the past round of revisions.

I will propose some broad suggestions that may enhance clarity and readability of the article, then address some specific amendments.

> Since the aim of this study is a modelling exercise, it would be nice to have a more rigorous model description. The model configuration is not very clear. It would be very helpful for the reader to see on the figure the initial and boundary conditions. On Fig. 4 as well, it would be very helpful to have these information present, as well as the highlight of the Vastness ridge.

Answer: We agree. In a previous version of the manuscript we had included a figure showing the model configuration, but that somehow slipped out.

Changes: *We added in the appendix a figure showing model configuration, and added spreading vectors to Figure 1. The crest of the Vestnesa Ridge is shown by the seismic line, as described in the caption.*

It would be very helpful for the reader to have a more structured result dissection and discussion. Maybe the authors could expose the full set of hypotheses and more quantitative facts in a first step, and then discuss and present their interpretation regarding the various aspects.

Changes: *we have changed the structure to have separated result and discussion sections. Please see above for details about the changes in the discussion. The discussion should reflect better what the state-of-knowledge is about seepage in the region and where does the importance of the tectonic hypothesis we present reside.*

Also, I would ask the authors to clearly distinguish between tectonic stress configuration optimal for enhanced fluid motion (extension regime) and actual mechanisms that may lead to flow focussing within chimneys and pockmarks. Fault planes will fail to produce pipe like features from a mechanical point of view.

Changes: *Thank you for rising this point. The relation between the chimneys and the faults/fractures is intriguing. Although the mechanical evolution of the gas chimneys escape the scope of the present study we extended the discussion about the spatial relation between faults and chimneys and touch upon the mechanical requirements to form a chimney. We offer a solution for a close spatial link between these two features.*

> The more specific comments are following:

L. 60-63: elastic stresses resulting from strain are instantaneous, thus I would be very careful using them to explain long term evolution and variations. They may be related to viscous creep rather than to purely elastic medium.

A: Thanks for pointing this out. In particular within the upper 50 m of sediments, the most recent interval through the gas chimneys towards the astern part of the ridge, have undulation features that remind features described in creep zones at other margins. However, there is a clear change with depth (from ca. 150 m) where the deformation is not expressed as chimneys but appear as near-vertical fault planes (documented in Plaza-Faverola et al). This paragraph was modified.

L. 73: please precise which fluids in the fluid dynamics you refer to.

A: done

L. 105-110: it is difficult to get the importance of the regional geology in the way it is brought to the reader. It would be very interesting to read about how these different geological formation impact the model, and the results.

A: The first section in the discussion links to the regional geological setting. The last 2 paragraphs were inserted in the discussion about the potential effect of tectonic stresses on near-surface faults.

L. 125-126: The last sentence is difficult to get, please rephrase.

A: done

L. 130: the GHSZ does not seem to be reported in Fig. 2, but rather in Fig. 3 ?

A: corrected

L. 134-138: What is the importance of those facts with regards to the proposed work ?

A: We have added a new reference here and elaborated on the idea for clarification. Thanks for pointing this out! The importance is that although the beginning of seepage is suspected to coincide with the onset of glaciations, the periodicity of the events does not correlate directly with either glacial or interglacials, but it seems to be more randomly controlled.

Section 4: Modelling approach. This section is about the aim of the paper, modelling. Thus, it would greatly benefit from enhanced details and a more rigorous model description, with regards to initial and boundary conditions especially.

A: A missing figure in the previous submission was re-inserted (appendix) and slightly edited. The appendix and the table in the supplementary material shall provide the necessary details about the modeling parameters.

L. 173: agreeing on the usage of a very simplified model, orientation of the stress field may be valid to interpret from the model, but I would be very careful regarding the magnitude of stresses, even if relative.

A: We reformulated for clarification. What we consider is rather the orientation of the principal stresses to determine the stress regime.

L. 210-213: Long and unclear sentence

A: Corrected.

L. 214: please precise style of principal stress

A: done

L. 218: please consider to rephrase avoiding the usage of “thing”

A: corrected. Apologies for that ☺

L. 219: please consider rephrasing as following “... provides a correct first order prediction of the stress field ORIENTATION in the upper crust...”

A: done: orientation and type

L. 221: consider the preferred usage of section number rather than below / above ...

A: corrected

L. 236: consider rephrasing “thicker sediment thickness” to make it more clear

A: corrected

L. 240: what is seismic definition ?

A: changed to: delineation of faults in the seismic

L. 268: Gravitationnel stress would not only induce the suggested stress, but a complex pattern.

A: Right, the discussion was re-structured and this part was reformulated.

L. 292 what unit is mm/a ?

A: millimeters per year. For some reason the glacial isostatic modeling folk and also in chronology it is often used "a". Must be from the latin annos. We changed to year

L. 234-235: Please make it clear to distinguish between tectonic stress that may enhance fluid circulation in specific location from the actually mechanism that will result in fluid localisation within pipes or chimneys. Faults and fractures will not be able to produce tubular like features, based on mechanics.

A: Thank you for pointing out this. Thinking about the distinction between chimneys and faults in terms of mechanics of fluids lead to further discuss about the timing of faulting vs. chimney formation. We have elaborated this idea further and introduced a couple of additional references.

L. 335: consider replacing above by the appropriate section number.

A: changed accordingly through the entire manuscript.

Fig. 2: missing BSR in legend ?

A: corrected

Fig. 4: add boundary conditions, highlight the Vestnesa Ridge

A: done

Based on the aforementioned arguments, I would suggest to publish this article but asking minor revision.

1 **CORRELATION BETWEEN TECTONIC STRESS REGIMES AND METHANE SEEPAGE ON THE
2 WEST-SVALBARD MARGIN**

3
4 A. Plaza-Faverola¹ and M. Keiding²

5 ¹ CAGE-Centre for Arctic Gas Hydrate, Environment, and Climate; Department of Geosciences, UiT The Arctic
6 University of Norway, N-9037 Tromsø, Norway

7 ² Geological Survey of Norway (NGU), P.O. Box 6315 Torgarden, 7491 Trondheim, Norway

8 *Correspondence to:* Andreia Plaza-Faverola (Andreia.a.faverola@uit.no)

9 **Abstract.** Methane seepage occurs across the west-Svalbard margin at water depths ranging from < 300 m,
10 landward from the shelf break, to > 1000 m in regions just a few kilometres away from the mid-ocean ridges in
11 the Fram Strait. The Vestnesa sedimentary ridge, located on oceanic crust at 1000-1700 m water depth, hosts a
12 perennial gas hydrate and associated free gas system. The restricted occurrence of acoustic flares to the eastern
13 segment of the sedimentary ridge, despite the presence of pockmarks along the entire ridge, indicates a spatial
14 variation in seepage activity. This variation coincides with a change in the faulting pattern as well as in the
15 characteristics of fluid flow features. Due to the position of the Vestnesa ridge with respect to the Molloy and
16 Knipovich mid-ocean ridges, it has been suggested that seepage along the ridge has a tectonic control. We
17 modelled the tectonic stress regime due to oblique spreading along the Molloy and Knipovich ridges to
18 investigate whether spatial variations in the tectonic regime along the Vestnesa Ridge are plausible. The model
19 predicts a zone of tensile stress that extends northward from the Knipovich Ridge and encompasses the zone of
20 acoustic flares on the eastern Vestnesa Ridge. In this zone the orientation of the maximum principal stress is
21 parallel to pre-existing faults. The model predicts a strike-slip stress regime in regions with pockmarks where
22 acoustic flares have not been documented. If a certain degree of coupling is assumed between deep crustal and
23 near-surface deformation, it is possible that ridge push forces have influenced seepage activity in the region by
24 interacting with the pore-pressure regime at the base of the gas hydrate stability zone. More abundant seepage on
25 the eastern Vestnesa Ridge at present may be facilitated by dilation of faults and fracture favourably oriented
26 with respect to the stress field. A modified state of stress in the past, for instance due to more significant glacial
27 stress, may have explained a more vigorous seepage activity along the entire Vestnesa Ridge. The contribution of
28 other mechanisms to the state of stress (i.e., sedimentary loading and lithospheric flexure) remain to be
29 investigated. Our study provides a first order assessment of how tectonic stresses may be influencing the
30 kinematics of near-surface faults and associated seepage activity offshore the west-Svalbard margin.

32

33 1. Introduction34 ~~Seafloor seepage is a wide spread phenomenon which consists in the release of natural gases into the oceans.~~35 Hundreds of gigatonnes of carbon are stored as gas hydrates and shallow gas reservoirs in continental margins
36 (e.g., Hunter et al., 2013). The release of these carbons over geological time, ~~a phenomenon known as methane~~
37 ~~seepage,~~ is an important ~~component of contribution to~~ the global carbon cycle. Understanding and quantifying
38 seepage has important implications for ocean acidification, deep-sea ecology and global climate. Periods of
39 massive methane release from gas hydrate systems (e.g., Dickens, 2011) or from large volcanic basins like that in
40 the mid-Norwegian Margin (e.g., Svensen et al., 2004) have been linked to global warming events such as the
41 Palaeocene-Eocene thermal maximum. ~~We know~~ It is well known that ~~methane~~ seepage ~~at continental margins~~
42 has been occurring ~~episodically~~ for millions of years (e.g., Judd and Hovland, 2009), but ~~we have~~ ~~there is~~ a poor
43 understanding of what forces it.

44

45 Present day seepage is identified as acoustic flares in the water column commonly originating at seafloor
46 depressions (e.g., Chand et al., 2012; Salomatin and Yusupov, 2011; Skarke et al., 2014; Smith et al.,
47 2014; Westbrook et al., 2009), while authigenic carbonate mounds are used as indicators of longer-term seepage
48 activity (e.g., Judd and Hovland, 2009). Seepage at the theoretical upstream termination of the gas hydrate
49 stability zone (GHSZ) (i.e., coinciding with the shelf edge) ~~at~~ different continental margins, has been explained
50 by temperature driven gas-hydrate dissociation (e.g., Skarke et al., 2014; Westbrook et al., 2009). On formerly
51 glaciated regions off Svalbard and the Barents Sea, active seepage has been explained by gas hydrate dissociation
52 either due to pressure changes resulting from the retreat of the ice-sheet (e.g., Portnov et al., 2016; Andreassen et
53 al., 2017) or to post-glacial uplift (Wallmann et al., 2018).

54

55 Across the west-Svalbard margin, active seepage extends beyond the shelf break and the region formerly covered
56 by ice. As a matter of fact, active seepage sites have been identified from inside Isfjorden (Roy et al., 2014) to
57 water depths of ~1200 m (Smith et al., 2014) where the Vestnesa Ridge hosts a perennially stable gas hydrate
58 system > 50 km seaward from the ice-sheet grounding line. The Vestnesa Ridge is a NW-SE oriented contourite
59 deposit located between the northward termination of the Knipovich Ridge and the eastern flank of the Molloy
60 spreading ridge in the Fram Strait (Fig. 1). Seafloor pockmarks along the Vestnesa Ridge, first documented by
61 Vogt et al., (1994), exist along the entire ridge. However, acoustic flares have been observed to originate
62 exclusively at large pockmarks located on the eastern part of the sedimentary ridge (Fig. 2, 3). A clear increase inFormatted: Font: (Default) +Headings (Times New Roman)
11 ptFormatted: List Paragraph, Numbered + Level: 1 +
Numbering Style: 1, 2, 3, ... + Start at: 1 + Alignment: Left +
Aligned at: 0,63 cm + Indent at: 1,27 cm

Formatted: Norwegian (Bokmål)

Field Code Changed

Formatted: Norwegian (Bokmål)

Field Code Changed

Formatted: Norwegian (Bokmål)

63 seepage activity towards the easternmost part of the ridge is thus evident from multiple year's water-column
64 acoustic surveys (Petersen et al., 2010;Bünz et al., 2012;Plaza-Faverola et al., 2017;Smith et al., 2014). In this
65 paper, we use the terminology "active" and "inactive" to differentiate between sites with and without documented
66 acoustic flares. Even though methane advection and methanogenesis are likely to be active processes along the
67 entire Vestnesa Ridge. The presence of inactive pockmarks—adjacent to a zone of active seepage—along the
68 Vestnesa Ridge, raises the question what stopped previously active seepage sites~~controls temporal and spatial~~
69 variations in seepage activity along the ridge?

70
71 Plaza-Faverola et al., (2015) documented seismic differences in the orientation and type of faulting along the
72 ridge and showed a link between the distribution of gas chimneys and faults. They hypothesised that seepage
73 activity may be explained by spatial variation in tectonic stress field across the margin (Plaza-Faverola et al.,
74 2015). However, the state of stress across Arctic passive margins has not been investigated. The total state of
75 stress at formerly glaciated continental margins can be the result of diverse factors including bathymetry and
76 subsurface density contrasts, subsidence due to glacial or sedimentary loading and lithospheric cooling.—in
77 addition to ridge-push forces (Fejerskov and Lindholm, 2000;Lindholm et al., 2000;Olesen et al., 2013;Stein et
78 al., 1989;Grunnaleite et al., 2009).
79
80

81 The interaction between the above mentioned factors renders modelling of the total state of stress a complex
82 problem that has not yet been tackled. In this study, we focus exclusively on the potential contribution of oblique
83 spreading at the Molloy and the Knipovich ridges to the total state of stress along the Vestnesa Ridge and do a
84 qualitative analysis of how teetonic stress~~stress~~ generated by mid-ocean ridge spreading may influence near-
85 surface faulting and associated seepage activity. The study of the effect of ridge push forces on near-surface
86 deformation across the west-Svalbard margin contributes to the current debate about neo-tectonism and stress
87 field variations across passive margins (Olesen et al., 2013;Salomon et al., 2015) and has implications for
88 understanding the mechanisms that control seepage at continental margins globally. Splay-faults are found to
89 drive fluid migration at subduction margins and to sustain shallow gas accumulations and seepage— (e.g.,
90 Plaza-Faverola et al., 2016;Minshull and White, 1989;Moore and Vrolijk, 1992;Crutchley et al., 2013), and the
91 relationship between fault kinematics and fluid migration has been documented specially at accretionary margins
92 where earthquake-induced seafloor seepage has been observed (e.g., Geersen et al., 2016). So far, the information
93 about the present day stress regime in the Fram Strait has been limited to large scale lithospheric density models

94 (Schiffer et al., 2018) and a limited number of poorly constrained stress vectors from earthquake focal
95 mechanisms (Heidbach et al., 2016). Our study provides a first order assessment of how stresses from slow
96 spreading mid-ocean ridges may be influencing the kinematics of near-surface faults and associated seepage
97 activity in an Arctic passive margin.

98

99 **4.2 Structural and stratigraphic setting**

100 In the Fram Strait, sedimentary basins are within tens of kilometres from ultra-slow spreading Arctic mid-ocean
101 ridges (Fig. 1). The opening of the Fram Strait was initiated 33 Ma ago and evolved as a result of slow spreading
102 of the Molloy and Knipovich Ridges (Engen et al., 2008). An important transpressional event deformed the
103 sedimentary sequences off western Svalbard, resulting in folds and thrustbelts, during the Paleocene-Eocene
104 dextral movement of Spitsbergen with respect to Greenland. Transpression stopped in the early Oligocene when
105 the tectonic regime became dominated by extension (Myhre and Eldholm, 1988). The circulation of deep water
106 masses through the Fram Strait started during the Miocene, ca. 17-10 Ma ago (Jakobsson et al., 2007; Ehlers and
107 Jokat, 2009), and established ~~the~~ the environmental conditions for the evolution of bottom current-driven
108 sedimentary drifts (Eiken and Hinz, 1993; Johnson et al., 2015). It has been suggested that the opening of the
109 northern Norwegian-Greenland Sea was initiated by the northward propagation of the Knipovich ridge into the
110 ancient Spitsbergen Shear Zone (Crane et al., 1991).

111

112 The continental crust beneath the western coast of Svalbard thins towards the Hornsund Fault zone indicating
113 extension following the opening of the Greenland Sea (Faleide et al., 1991). Late Miocene and Pliocene
114 sedimentation, driven by bottom currents, resulted in the formation of the ca. 100 km long Vestnesa Ridge
115 between the shelf break off west-Svalbard and oceanic crust highs at the eastern flank of the Molloy mid-ocean
116 ridge (Eiken and Hinz, 1993; Vogt et al., 1994). The sedimentary ridge is oriented parallel to the Molloy
117 Transform Fault and its crest experiences a change in morphology from being narrow on the eastern segment to
118 be more like a plain expanded broader on the western Vestnesa Ridge segment (Fig. 2). The exact location of the
119 continental-ocean transition remains somewhat uncertain (Eldholm et al., 1987) but it is inferred to be nearby the
120 transition from the eastern to the western segments (Engen et al., 2008).

121

122 The total sedimentary thickness along the Vestnesa Ridge remains unconstrained. Based on one available
123 regional profile it can be inferred that the ridge is > 5 km thick in places (Eiken and Hinz, 1993). It has been
124 divided into three main stratigraphic units (Eiken and Hinz, 1993; Hustoft, 2009): the deepest sequence, YP1,

125 consists of synrift and post-rift sediments deposited directly on oceanic crust; YP2 consists of contourites; and
126 YP3, corresponding to the onset of Pleistocene glaciations (ca. 2.7 Ma ago) (Mattingdal et al., 2014), is a mix of
127 glaciomarine contourites and turbidites. The effect of ice-sheet dynamics on the west-Svalbard margin (Patton et
128 al., 2016;Knies et al., 2009) has influenced the stratigraphy, and most likely the morphology, of the Vestnesa
129 Ridge and adjacent sedimentary basins. In this Arctic region, glaciations are believed to have started even earlier
130 than 5 Ma ago. The local intensification of glaciations is inferred to have started ca. 2.7 Ma ago (e.g., Faleide et
131 al., 1996;Mattingdal et al., 2014). Strong climatic fluctuations characterized by intercalating colder, intense
132 glaciations with warmer and longer interglacials, dominated the last ca. 1 Ma. (e.g., Jansen et al., 1990;Jansen
133 and Sjøholm, 1991).

134

135 ~~A set of N-S to NNE-SSE trending faults cut the recent strata at a narrow zone between the Vestnesa Ridge and~~
136 ~~the northern termination of the Knipovich Ridge (Fig 1). Due to their structural connection with the Knipovich~~
137 ~~Ridge they have been suggested to indicate ongoing northward propagation of the rift system~~ (Crane et al.,
138 2001;Vanneste et al., 2005). High resolution 3D seismic data collected on the eastern Vestnesa Ridge revealed
139 ~~sub seafloor NW-SE oriented faults (i.e., near vertical and parallel to the sedimentary ridge axis) that could be~~
140 ~~genetically associated with the outcropping faults (Plaza Faverola et al., 2015; Fig. 2). Comparison of similar~~
141 ~~high resolution 3D seismic data from the western Vestnesa Ridge shows that the style of faulting has been~~
142 ~~radically different from that of the eastern segment. Here, only randomly oriented short fault segments are~~
143 ~~revealed in nevertheless pockmarked Holocene strata (Fig. 2).~~

Commented [AAPF1]: Moved to be integrated in the discussion

144

145 ~~The gas hydrate system dynamics along the Vestnesa Ridge seems to be highly influenced by spatial variations in~~
146 ~~the geothermal gradient and the gas composition (Plaza-Faverola et al., 2017). Thermogenic gas accumulations at~~
147 ~~the base of the GHSZ (Fig. 2) are structurally controlled (i.e., the gas migrates towards the crest of the~~
148 ~~sedimentary drift) and part of this gas sustains present day seepage activity (Bünz et al., 2012;Plaza-Faverola et~~
149 ~~al., 2017;Knies et al., 2018). Reservoir modelling shows that source rock deposited north of the Molloy~~
150 ~~Transform Fault has potentially started to generate thermogenic gas 6 Ma ago and that migrating fluids reached~~
151 ~~the Vestnesa Ridge crest at the active seepage site ca. 2 Ma ago (Knies et al., 2018). It is suspected that seepage~~
152 ~~has been occurring, episodically, at least since the onset of the Pleistocene glaciations c. 2.7 Ma ago leaving~~
153 ~~buried pockmarks and authigenic carbonate crusts as footprint (Plaza-Faverola et al., 2015)–(Schneider et al.,~~
154 ~~2018a)Many transient seepage events are suspected and one was dated to ca. 17.000 years based on the presence~~

155 ~~of a 1000 years old methane dependent bivalve community possibly sustained by a gas pulse through a fault~~
156 (Ambrose et al., 2015)-

157

158 2.3. Seismic data

159 The description of faults and fluid flow related features along the Vestnesa Ridge is documented ~~in by several~~
160 authors (Bünz et al., 2012; Hustoft, 2009; Petersen et al., 2010; Plaza-Faverola et al., 2015; Plaza-Faverola et al.,
161 2017) ~~Plaza-Faverola et al., 2015. The description is based on~~ Two-3D high resolution seismic data sets acquired
162 on the western and the eastern Vestnesa Ridge respectively (Fig. 2), and one 2D seismic line acquired along the
163 entire Vestnesa Ridge extent ~~have been particularly useful in the description of the structures along the ridge~~ (Fig.
164 5). These data have been previously used for the investigation of the bottom simulating reflection dynamics (i.e.,
165 the seismic indicator of the base of the gas hydrate stability zone) (Plaza-Faverola et al., 2017) and
166 documentation of gas chimneys and faults in the region (Petersen et al., 2010; Plaza-Faverola et al., 2015; Bünz et
167 al., 2012). The data were acquired on board R/V Helmer Hanssen using the 3D P-Cable system (Planke et al.,
168 2009). Final lateral resolution of the 3D data sets is given by a bin size of $6.25 \times 6.25 \text{ m}^2$ and the vertical resolution
169 is $> 3 \text{ m}$ with a dominant frequency of 130 Hz. Details about acquisition and processing can be found in Petersen
170 et al., 2010 and Plaza-Faverola et al., 2015. For the 2D survey the dominant frequency was $\sim 80 \text{ Hz}$ resulting in a
171 vertical resolution $> 4.5 \text{ m}$ (assumed as $\lambda/4$ with an acoustic velocity in water of 1469 m/s given by CTD data;
172 Plaza-Faverola et al., 2017).

173

174 3.4. The modelling approach

175 The modelling carried out in this study deals exclusively with tectonic stress due to ridge push. We use the
176 approach by Keiding et al. (2009) based on the analytical solutions derived by Okada (1985), to model the plate
177 motion and tectonic stress field due to spreading along the Molloy and Knipovich Ridges.

178

179 The Okada model and our derivation of the stress field from it is described in more detail in appendix A. The
180 Molloy and Knipovich Ridges are modelled as rectangular planes with opening and transform motion in a flat
181 Earth model with elastic, homogeneous, isotropic rheology (Fig. A1 in appendix). Each rectangular plane is
182 defined by ten model parameters used to approximate the location, geometry and deformation of the spreading
183 ridges (Okada, 1985; see supplement Table 1). The locations of the two spreading ridges were constrained from
184 bathymetry maps (Fig. 1). The two spreading ridges are assumed to have continuous, symmetric deformation
185 below the brittle-ductile transition, with a half spreading rate of 7 mm/yr and a spreading direction of N125°E,

Formatted: Font: Bold, Not All caps

Formatted: Font: Bold, Not All caps

186 according to recent plate motion models (DeMets et al., 2010). Because the spreading direction is not
187 perpendicular to the trends of the spreading ridges, this results in both opening and right-lateral motion; that is,
188 oblique spreading on the Molloy and Knipovich Ridges. The Molloy Transform Fault, which connects the two
189 spreading ridges, trends N133°E, thus a spreading direction of N125°E implies extension across the transform
190 zone. We use a depth of 10 km for the brittle-ductile transition and 900 km for the lower boundary of the
191 deforming planes, to avoid boundary effects. For the elastic rheology, we assume typical crustal values of
192 Poisson's ratio = 0.25 and shear modulus = 30 GPa (Turcotte and Schubert, 2002). We perform sensitivity tests
193 for realistic variations in [1\) model geometry](#) [24\) spreading direction](#), [32\) depth of the brittle-ductile transition](#),
194 [and 43\) Poisson's ratio](#) -(Supplementary material). Variations in shear modulus, e.g. reflecting differences in
195 elastic parameters of crust and sediments, would not influence the results, because we [do not consider the](#)
196 [magnitude of the stresses](#).

197

198 Asymmetric spreading has been postulated for the Knipovich Ridge based on heat flow data (Crane et al., 1991),
199 and for other ultraslow spreading ridges based on magnetic data (e.g., Gaina et al., 2015). However, the evidence
200 for asymmetry along the Knipovich Ridge remains inconclusive and debatable in terms, for example, of the
201 relative speeds suggested for the North American (faster) and the Eurasian (slower) plates (Crane et al.,
202 1991;Morgan, 1981;Vogt et al., 1994). This reflects that the currently available magnetic data from the west-
203 Svalbard margin is not of a quality that allows an assessment of possible asymmetry of the spreading in the Fram
204 Strait (Nasuti and Olesen, 2014). Symmetry is thus conveniently assumed for the purpose of the present study.

205

206 We focus on the stress field in the upper part of the crust (where the GHSZ is) and characterise the stress regime
207 based on the [relative magnitudes of the relationship between the](#) horizontal and vertical stresses. We refer to the
208 stresses as σ_v (vertical stress), σ_H (maximum horizontal stress) and σ_h (minimum horizontal stress), where
209 compressive stress is positive (Zoback and Zoback, 2002). A tensile stress regime ($\sigma_v > \sigma_H > \sigma_h$) favours the
210 opening of steep faults that can provide pathways for fluids. Favourable orientation of stresses with respect to
211 existing faults and/or pore fluid pressures increasing beyond hydrostatic pressures are additional conditions for
212 leading to opening for fluids under strike-slip ($\sigma_H > \sigma_v > \sigma_h$) and compressive ($\sigma_H > \sigma_h > \sigma_v$) regimes (e.g.,
213 Grauls and Baleix, 1994).

214

215 [5. Results and discussion](#)

Commented [AAPF2]: Separation between results and discussion sections

Formatted: Not All caps

Formatted: Not All caps

216 **5.1 Predicted type and orientation of stress fields due to oblique spreading at the Molloy and the Knipovich
217 ridges**

Formatted: Not All caps

218 The model predicts zones of tensile stress near the spreading ridges, and strike-slip at larger distances from the
219 ridges. An unexpected pattern of tensile stress arises from the northward termination and the southward
220 termination of the Knipovich and Molloy ridges respectively (Fig. 3). -The zone of tensile stress that extends
221 northward from the Knipovich Ridge, encompassesing the eastern part of the Vestnesa Ridge. The western
222 Vestnesa Ridge, on the other hand, lies entirely in a zone of strike-slip stress (Fig. 3). The sensitivity tests show
223 that the tensile stress zone is a robust feature of the model, that is, variations in the parameters result in a change
224 of the extent and shape of the tensile zone but the zone remains in place (Supplementary material). It appears that
225 the tensile zone is a result of the interference of the stress from the two spreading ridges. To illustrate this, we ran
226 the model for the Molloy Ridge and the Knipovich Ridge independently. In the model with Knipovich Ridge
227 alone, a large tensile zone extends northeast from the ridge's northern end, covering only the easternmost part of
228 Vestnesa Ridge (Fig. 4). Under the influence of the strike-slip field from the Molloy Ridge, this zone is deflected
229 and split into two lobes, of which one extends to the eastern Vestnesa Ridge.

Commented [AAPF3]: Addition based on the sensitivity test for geometry changes

Formatted: Font: 11 pt

230
231 To investigate the geometric relationship between the predicted stress field and mapped faults, we calculated the
232 orientations of maximum compressive horizontal stress (Lund and Townend, 2007). The maximum horizontal
233 stresses (σ_H) approximately align with the spreading axes within the tensile regime and are perpendicular to the
234 axes within the strike-slip regime (Fig. 3). Spreading along the Molloy ridge causes NW-SE orientation of the
235 maximum compressive stress along most of the Vestnesa Ridge, except for the eastern segment where the
236 influence of the Knipovich Ridge results in a rotation of the stress towards E-W (Fig. 3).

237

238 The simplifying assumptions involved in our model imply that the calculated stresses in the upper crust are
239 unconstrained to a certain degree. However, the predicted stress directions are in general agreement with other
240 models of plate tectonic forces (e.g., Gölke and Coblenz, 1996; Naliboff et al., 2012). In addition, and Árnadóttir
241 et al. (2009) demonstrated that the deformation field from the complex plate boundary in Iceland could be
242 modelled using Okada's models. More importantly, a comparison of the predicted strike-slip and tensile stress
243 fields from plate spreading and observed earthquake focal mechanisms shows an excellent agreement, both with
244 regards to style stress regime and orientation of principal stressesmaximum compressive stress. The earthquake
245 focal mechanisms are mostly normal along the spreading ridges and strike-slip along the transform faults, and the
246 focal mechanism pressure axes align nicely with the predicted directions of maximum compressive stress (Fig.

247 3). The good agreement between Okada's model and other modelling approaches as well as between the resulting
248 stresses and focal mechanisms in the area ~~indicates two things~~^{indicates} : 1. that the model, despite the simplicity
249 of its assumptions, provides a correct first order prediction of ~~orientation and type of the~~ stress field in the
250 upper crust, ~~and 2. that stress from plate spreading may be transferred~~ have a significant influence ~~towards the~~
251 ~~near surface sediments influencing~~ on the state of stress~~deformation~~ along the Vestnesa Ridge. (Other possible
252 sources of stress in the region will be discussed in more detail ~~in section 6.1~~^{in section 6.1} below. It remains an open
253 question to which degree the crustal stresses are transferred to the sedimentary successions of the Vestnesa
254 Ridge. For compacted stratigraphic formations in the Norwegian Sea, a comparison of shallow *in situ* stress
255 measurements and deeper observations from earthquake focal mechanisms indicates that the stress field is
256 homogeneous in direction over a large depth range (Fejerskov and Lindholm, 2000). For an overburden
257 constituted of Quaternary sediments, though, the stress coupling between the crust and the near-surface depends
258 on the shear strength of the sediments. The upper 200 m of hemipelagic sediment along the Vestnesa Ridge
259 are relatively young (< 2 Ma) and is not expected to be highly consolidated. However, the fact that a large number
260 of faults extend several hundred meters through the sediments suggests that compaction of the sediments has
261 been large enough to build up some amount of shear strength. Geotechnical studies from different continental
262 margins indicate that deep marine sediments can experience high compressibility due to the homogeneity in the
263 grain structure (i.e., large areas made of a single type of sediment), providing favourable conditions for shear
264 failure (Urlaub et al., 2015; DeVore and Sawyer, 2016). We, therefore, consider it possible that the upper
265 sediments along the Vestnesa Ridge can be deformed by tectonic stress.

266
267 **5.2 Distribution of fault~~sing~~ and seepage activity along the Vestnesa Ridge with respect to modelled**
268 **tectonic stress**

269
270 High-resolution 3D seismic data collected on the eastern Vestnesa Ridge revealed sub-seabed NW-SE oriented,
271 near-vertical faults with a gentle normal throw (< 10 m). In this part of the Vestnesa Ridge, gas chimneys and
272 seafloor pockmarks are ca. 500 m in diameter. On structural maps extracted along surfaces within the gas hydrate
273 stability zone (GHSZ) gas chimneys project over fault planes or at the intersection between fractures (Fig. 2). The
274 faults mapped in this part of the ridge structures mapped could be genetically associated with a^A set of N-S to
275 NNE-SSE trending faults that outcrop at the seafloor at a narrow zone between the Vestnesa Ridge and the
276 northern termination of the Knipovich Ridge (Fig 1, 2). These faults could be genetically associated with the
277 faults on the crest of Vestnesa Ridge (Plaza-Faverola et al., 2015; Fig. 2), but they have also^{Due to their}

278 structural connection with the Knipovich Ridge the outerropping faults have been suggested to indicate ongoing
279 northward propagation of the Knipovich rift system (Crane et al., 2001;Vanneste et al., 2005).
280

281 Most of the outcropping N-S to NNE-SSE oriented faults north of the Knipovich Ridge and the sub-seafloor NW-
282 SE oriented faults on the eastern Vestnesa Ridge are located within the zone of modelled tensile regime that
283 extends northward from the Knipovich Ridge (Fig. 3). The orientation of σ_H rotates from being perpendicular to
284 the Molloy ridge nearby sub-seafloor faults at the eastern Vestensa Ridge, to be perpendicular to the Knipovich
285 Ridge in places within the tensile zone (Fig. 3). Interestingly, documented acoustic flares along the Vestensa
286 Ridge are also located within the zone of modelled tensile stress regime (Fig. 3). -The match between the extent
287 of the modelled tensile zone and the active pockmarks is not exact; active pockmarks exist a few kilometres
288 westward from the termination of the tensile zone (Fig. 3). However, the agreement is striking from a regional
289 point of view. Some of the outcropping faults north of the Knipovich Ridge and south of the Molloy transform
290 fault appear located outside the modelled tensile zone (Fig. 3; Fig. S1-S4 in the supplement). Inactive pockmarks
291 (i.e., no acoustic flares have been observed during several visits to the area) are visible on high resolution
292 bathymetry maps over these faulted regions (Dumke et al., 2016;Hustoft, 2009;Johnson et al., 2015;Waghorn et
293 al., 2018).
294

295 In a similar high-resolution 3D seismic data set from the western Vestnesa Ridge the faults have different
296 characteristics compared to those of the eastern segment. In this part of the ridge gas chimneys are narrower,
297 buried pockmarks are stacked more vertically than the chimneys towards the east and it is possible to recognise
298 more faults reaching the present-day seafloor (Plaza-Faverola et al., 2015). Fault segments are more randomly
299 oriented with a tendency for WNW-ESE and E-W orientations (Fig. 2). These structures coincide with a
300 modelled strike-slip stress regime with σ_H oriented nearly perpendicular to the Molloy Ridge (Fig. 3).
301
302
303

304 6. Discussion

Formatted: Font: Bold

305 The striking correlation coincidence between the spatial variation in predicted tensile modelled stress regimes
306 and the pattern of faulting and seepage activity along the Vestnesa Ridge leads to the discussion whether -
307 tectonic stresses resulting from plate oblique spreading at the Molloy and the Knipovich ridges - have the potential
308 to influence near-surface -deformation and fluid dynamics in the study area. We discuss first the modelling results

309 in the context of the total state of stress across passive margins and to which extent regional stresses can
310 influence near-surface deformation. Assuming that tectonic stress can potentially influence near-surface
311 deformation, we discuss then the effect that the modelled stress fields would have on pre-existing faults and
312 associated fluid migration. Finally, we propose a model for explaining seepage evolution along the Vestnesa
313 Ridge coupled to stress field variations. We close the discussion with a note on the implications of the present
314 study for understanding near-surface fluid dynamics across passive margins globally.

315

316 **6.1 Modelled stress in the context of the total state of stress along the Vestnesa Ridge**

317 Since In this study we focused exclusively on modelling the type and orientation of stresses potentially generated
318 by oblique spreading at the Molloy and Knipovich ridges, and we have Other sources of stress have been so far
319 disregarded, any other source of stress. Hence, the modelled stress field documented in this study cannot be
320 understood as a representation of the total state of stress in the region. Modelling studies from Atlantic-type
321 passive margins, suggest that from all the possible sources of stress across passive margins (i.e., sediment
322 loading, glacial flexure, spatial density contrasts, and ridge push as well as basal drag forces) sediment loading
323 (assuming elastic deformation) appears to be the mechanism with the potential of generating the largest
324 magnitudes of stresses across passive margins (Stein et al., 1989; Turcotte et al., 1977). However, stress
325 information derived from seismological and in-situ data (Fjeldskaar and Amantov, 2018; Grunnalite et al.,
326 2009; Lindholm et al., 2000; Olesen et al., 2013) and paleo-stress field analyses based on dip and azimuth of fault
327 planes (Salomon et al., 2015) point towards a dominant effect of ridge push forces on the state of stress across
328 passive continental margins. Given the proximity of the Vestnesa Ridge to the Molloy and the Knipovich ridges
329 (Fig. 1), we argue that tectonic stress from spreading can be an important factor, perhaps even a dominant factor,
330 controlling near-surface deformation along the Vestnesa Ridge.

331

332 The contemporary stress field across the west-Svalbard passive margin is presumably the result of an interaction
333 between large-scale tectonic stress mechanisms (i.e., ridge push, basal drag) overprinted by regional (i.e., density
334 contrasts, glacial related flexure, sediment loading) and local mechanisms (e.g., topography, pore-fluid pressure
335 variations, faulting). In the concrete case of the Vestnesa Ridge, a change in the faulting pattern, the distribution
336 of shallow gas and gas hydrates, as well as differences in the topographic characteristics of the ridge crest (Fig.
337 2), are all factors likely to induce local changes in near-surface stress. We discuss in the following sections how
338 local stress-generating mechanisms may interact with tectonic forcing to control fluid dynamics and seepage.

339

Formatted: Font: (Default) +Headings (Times New Roman), 11 pt, Bold

Formatted: List Paragraph, Outline numbered + Level: 2 + Numbering Style: 1, 2, 3, ... + Start at: 1 + Alignment: Left + Aligned at: 0 cm + Indent at: 0,63 cm

Formatted: Font: (Default) +Headings (Times New Roman), 11 pt, Bold

Formatted: Font: (Default) +Headings (Times New Roman), 11 pt, Bold

340 The Vestnesa sedimentary Ridge sits over relatively young oceanic crust, < 19 Ma old (Eiken and Hinz,
341 1993; Hustoft, 2009). The oceanic-continental transition is not well constrained but its inferred location crosses
342 the Vestnesa Ridge at its easternmost end (Engen et al., 2008; Hustoft, 2009). This is a zone prone to flexural
343 subsidence due to cooling during the evolution of the margin and the oceanic crust may have experienced syn-
344 sedimentary subsidence nearby the oceanic-continental transition, as suggested for Atlantic passive margins
345 (Turcotte et al., 1977). However, syn-sedimentary subsidence would result in N-S oriented faults (i.e., reflecting
346 the main direction of major rift systems during basin evolution) (Faleide et al., 1991; Faleide et al., 1996).
347 Although one N-S oriented fault outcrops in bathymetry data at the transition from the eastern to the western
348 Vestnesa Ridge segments (Fig. 5a), most of the sub-seabed faults and associated fluid migration features in 3D
349 seismic data are~~The~~ NW-SE to E-W oriented (Fig. 1, 2) faults on the Vestnesa Ridge point towards a different
350 origin. Similarly, the weight of the contourite ridge over the oceanic crust may have generated additional stress
351 on the Vestnesa Ridge. However, for a sedimentary load to generate large contemporaneous stress sedimentation
352 would need to occur at fast rates (e.g., > 1 mm/year) so the stress builds up faster than it relaxes at the crust (Stein
353 et al., 1989). Sedimentation rates on the Vestnesa Ridge are estimated to have fluctuated between 0.1-0.6
354 mm/year since the onset of glaciations 2.7 Ma ago (Plaza-Faverola et al., 2017; Knies et al., 2018; Mattingdal et
355 al., 2014).

Formatted: English (United States)

356
357 Glacial isostasy results in significant stresses associated with flexure of the lithosphere as the ice-sheet advances
358 or retreats. Present uplift rates are highest at the centre of the formerly glaciated region where the ice thickness
359 was at the maximum (Fjeldskaar and Amantov, 2018). Modelled present day uplift rates at the periphery of the
360 Barents sea ice-sheet ranges from 0 to -1 mm/year, depending on the ice-sheet model used in the calculation
361 (Auriac et al., 2016) compared to an uplift rate of up to 9 mm/year at the centre of the ice sheet (Auriac et al.,
362 2016; Patton et al., 2016). Modelled glacial stresses induced by the Fennoscandian ice sheet on the mid-
363 Norwegian margin are close to zero at present day (Lund et al., 2009; Steffen et al., 2006). By analogy, present
364 day stress at the Vestnesa Ridge - located ~60 km from the shelf break - may be insignificant. It is likely that
365 glacial stresses as far off as the Vestnesa Ridge had a more significant effect in the past, as further discussed in
366 section 6.3 and 6.4.

367 **6.3**

368

369 Finally, spreading ridge push forcing has the potential of being a dominant factor on the state of stress across the
370 west-Svalbard margin as observed for Norwegian margins (Fejerskov and Lindholm, 2000; Lindholm et al.,

371 2000). Specifically, the Vestnesa Ridge has the particularity that it is located within the expected range of
372 maximum influence of ridge push forces on the stress regime (Fejerskov and Lindholm, 2000) and that forces
373 from two spreading ridges influence it from different directions (i.e., the Molloy Ridge from the west and the
374 Knipovich Ridge from the south-east). The intriguing stress pattern appears to be caused by the interaction of the
375 stress generated by the two spreading ridges, as described above (section 5.1).

376

377 |

378 6.2 Effect of the modelled stress fields on pre-existing faults and present day seepage

379

380 Bearing in mind that several factors contribute to the total state of stress at different scales across passive margins
381 we assume that an influence on near-surface deformation by mid-ocean ridge stresses is plausible and discuss
382 their potential effect on seepage activity. Depending on the tectonic regime, the permeability through faults and
383 fractures may be enhanced or inhibited (e.g., Sibson, 1994; Hillis, 2001; Faulkner et al., 2010). Thus, spatial and
384 temporal variations in the tectonic stress regime may control the transient release of gas from the seafloor over
385 geological time as documented, for example, for CO₂ analogues in the Colorado Plateau (e.g., Jung et al., 2014).

386

387 A gas hydrate system is well developed and shallow gas accumulates at the base of the GHSZ along the entire
388 Vestnesa Ridge (Plaza-Faverola et al., 2017). Thermogenic gas accumulations at the base of the GHSZ (Fig. 5)
389 are structurally controlled (i.e., the gas migrates towards the crest of the sedimentary drift) and together with
390 microbial methane this gas sustains present day seepage activity (Bünz et al., 2012; Plaza-Faverola et al.,
391 2017; Knies et al., 2018). All the conditions are given for sustaining seepage along the entire ridge. However,
392 seepage is focused and restricted. Some of the mechanisms commonly invoked to explain seepage activity across
393 passive margins include climate related gas hydrate dissociation, tidal or seasonal sea-level changes, and pressure
394 increases in shallow reservoirs due to fast sedimentation - (e.g., Bünz et al., 2003; Hustoft et al., 2010; Karstens et
395 al., 2018; Riboulot et al., 2014; Skarke et al., 2014; Berndt et al., 2014; Wallmann et al., 2018; Westbrook et al.,
396 2009; Franek et al., 2017). While all of these mechanisms may influence to a certain degree seepage systems as
397 deep as the Vestnesa Ridge (> 1000 m deep; as discussed further in section 6.3) they offer no explanation as to
398 why seepage activity is more substantial within chimney sites proximal to or at fault planes and why seepage is at
399 a minimum or stopped elsewhere along the ridge (Fig. 2). Overall, the pattern of seepage activity along the
400 Vestnesa Ridge is strikingly consistent with the modelled tectonic stress field pattern. Acoustic flares have been
401 documented to originate from < 10 m broad zones (Panieri et al., 2017) within pockmarks located exclusively

Formatted: Font: (Default) +Headings (Times New Roman), 11 pt

Formatted: List Paragraph, Outline numbered + Level: 2 + Numbering Style: 1, 2, 3, ... + Start at: 1 + Alignment: Left + Aligned at: 0 cm + Indent at: 0,63 cm

Formatted: Font: (Default) +Headings (Times New Roman), 11 pt

Formatted: Font: (Default) +Headings (Times New Roman), 11 pt

402 along faults. We suggest that these faults are favourably oriented with respect to a tectonic σ_H (Fig. 2) and that
403 opening of fault segments favourably oriented with respect to the stress field is one controlling factor of present
404 day seepage.

405
406 Present day seepage activity is less favourable pronounced towards the western Vestnesa Ridge. Despite available
407 gas trapped at the base of the GHSZ (Fig. 5) the faults are generally less favourably oriented for tensile opening
408 (i.e., NW-SE oriented σ_H) and are under a strike-slip regime (Fig. 2). The cluster of larger scale N-S to NNW-
409 SSE trending extensional faults that outcrop at the southern slope of the Vestnesa Ridge (Fig. 1, 2), also coincides
410 with the zone of predicted tensile stress (Fig. 3). However, the modelled maximum compressive stress in this area
411 is generally oblique to the fault planes (Fig. 3), making these faults less open for gas. Interestingly, this is also a
412 zone of pockmarks where acoustic flares have not been observed (e.g., Johnson et al., 2015; Hustoft et al., 2009;
413 Vanneste et al., 2005). A set of N-S oriented structures south of the Molloy Transform Fault and a train of
414 pockmarks at the crest of a ridge west of the Knipovich Ridge axis are located under a strike-slip regime with N-
415 S oriented σ_H (Fig. 3). Although gas accumulations and gas hydrates have been identified at the crest of this
416 ridge, acoustic flares have so far not been documented in the region (Johnson et al., 2015; Waghorn et al., 2018).

417 We suggest that the N-S trending faults in this region may be impermeable for fluids despite a parallel σ_H , if the
418 stress regime is transpressive. Transpression has been documented at different stages of opening of the Fram
419 Strait (Jokat et al., 2016) and is thus a plausible tectonic mechanism for holding the gas from escaping. Ongoing
420 studies will shed light into the structural evolution of this near-surface system.

421
422 The bathymetry of the southern flank of the Vestnesa Ridge deepens from 1200-1600 m along the crest of the
423 Vestnesa Ridge to ca. 2000 m near the Molloy Transform Fault (Fig. 1). Thus, an additional effect of
424 gravitational stress on near-surface deformation and seepage in the region cannot be ruled out. In particular,
425 although the faults at the steep slope north of the Knipovich Ridge have been suggested to reflect the northward
426 propagation of the Knipovich Ridge rift system (Crane et al., 2001; Vanneste et al., 2005), it is likely that their
427 formation was influenced by gravitational stresses. Small-scale slumps at the slope (Fig. 1, 2) could be also
428 evidence of gravitational forcing at the steep southern flank of the Vestnesa Ridge. However, sub-seabed faults
429 on the eastern Vestnesa Ridge dip towards the NE (Fig. 5c), suggesting that gravitational forcing is not
430 necessarily influencing the behaviour of faults and current seepage activity on the eastern Vestnesa Ridge.

431
432 6.3 Seepage evolution coupled to stress field variations

Formatted: Font: (Default) +Headings (Times New Roman),
11 pt

Formatted: List Paragraph, Outline numbered + Level: 2 +
Numbering Style: 1, 2, 3, ... + Start at: 1 + Alignment: Left +
Aligned at: 0 cm + Indent at: 0,63 cm

433
434 The seepage systems along the Vestnesa Ridge has been highly dynamic over geological time. Both microbial
435 and thermogenic gas contribute to the gas hydrate and seepage system (Hong et al., 2016;Panieri et al.,
436 2017;Plaza-Faverola et al., 2017;Smith et al., 2014). Reservoir modelling shows that source rock deposited north
437 of the Molloy Transform Fault has potentially started to generate thermogenic gas 6 Ma ago and that migrating
438 fluids reached the Vestnesa Ridge crest at the active seepage site ca. 2 Ma ago (Knies et al., 2018). Seepage has
439 been occurring episodically, at least since the onset of the Pleistocene glaciations directly through faults, and a
440 deformation typical of gas chimneys (i.e., where periodicity is evidenced by buried pockmarks and authigenic
441 carbonate crusts) -seems to have started later (Plaza-Faverola et al., 2015). However, the periodicity of seepage
442 events documented since the Last Glacial Maximum seems to correlate indistinctively with glacials or
443 interglacials (Consolaro et al., 2015;Schneider et al., 2018a;Sztybor and Rasmussen, 2017). One transient event
444 was dated to ca. 17.000 years based on the presence of a ~1000 years old methane-dependent bivalve community
445 possibly sustained by a gas pulse through a fault or chimney (Ambrose et al., 2015). A tectonic control on the
446 evolution of near-surface fluid flow systems and seepage along the Vestnesa Ridge is an explanation that
447 reconciles the numerous cross-disciplinary observations in the area.

448
449 The spatial relation between gas chimneys at the crest of the ridge and fault planes (Fig. 2, 3c) (Bünz et al.,
450 2012;Plaza-Faverola et al., 2015) is intriguing and raises the question whether the faulting was posterior to
451 brecciation (fracturing) of the strata during chimney formation. Gas chimneys form by hydrofracturing generated
452 at a zone of overpressure in a reservoir (e.g., Karstens and Berndt, 2015;Hustoft et al., 2010 and references
453 therein;Davies et al., 2012). From the mechanical point of view the tensile faults at the eastern Vestnesa Ridge
454 would not be a favourable setting for the generation of hydrofracturing and chimney formation right at the fault
455 planes as observed in the seismic (Fig. 2, 3c). For gas chimneys to be the youngest features fault segments would
456 have to become tight and permeable at certain periods of times, allowing pore fluid pressure at the free gas zone
457 beneath the GHSZ to build up (Fig. 5). This is a plausible scenario. The faults may get locally plugged with gas
458 hydrates and authigenic carbonate and activated a self-sealing mechanism similar to that suggested for chimneys
459 at other margin (e.g., Hovland, 2002). Nevertheless, where gas chimneys do not disturb the seismic response,
460 fault planes are observed to extend near the seafloor (Fig. 5c). This observation suggests that latest faulting
461 periods may have broken through already brecciated regions connecting thus gas chimneys that were already in
462 placed. Both cases are consistent with the fact that -acoustic flares and seepage bubbles are restricted to focused
463 weakness zones (Panieri et al., 2017). We suggest that an interaction between pore fluid pressure at the base of

464 the GHSZ and tectonic stress has led to local stress field variations and controlled seepage evolution. Opening of
465 fractures is facilitated if the minimum horizontal stress is smaller than the pore-fluid pressure (p_f), that is, the
466 minimum effective stress is negative ($\sigma_h' = \sigma_h - p_f < 0$) (e.g., Grauls and Baleix, 1994). Secondary permeability
467 may increase by formation of tension fractures near damaged fault zones (Faulkner et al., 2010). Cycles of
468 negative minimum effective stress and subsequent increase in secondary permeability in a tensile stress regime
469 can be achieved particularly easy in the near-surface and would provide an explanation for the development of
470 chimneys coupled to near-surface tectonic deformation. A constant input of thermogenic gas from an Eocene
471 reservoir since at least ca. 2 Ma ago would have contributed to localized pore-fluid pressure increases (Knies et
472 al. 2018).

473
474 Geophysical and paleontological data indicate that there was once more prominent seepage and active chimney
475 development on the western Vestnesa Ridge segment (e.g., Consolaro et al., 2015; Plaza-Faverola et al.,
476 2015; Schneider et al., 2018b). An interaction between pore-fluid pressure and tectonic stress would explain
477 variations in the amount of seepage activity over geological time. Following the same explanation as for the
478 present day seepage, the negative σ_h' condition could have been attained anywhere along the Vestensa Ridge in
479 the past due to pore fluid pressure increases at the base of the GHSZ or due to favourable stress conditions.
480 During glacial periods, flexural stresses should have been significantly higher than at present day (Lund and
481 Schmidt, 2011). According to recent models of glacial isostasy by the Barents Sea Ice sheet during the last glacial
482 maximum, the Vesntesa Ridge laid in a zone where subsidence could have been of tens of meters (Patton et al.,
483 2016). At other times, before and after glacial maximums, the Vestnesa Ridge was possibly located within the
484 isostatic forebulge.

485
486 In general, it is expected that maximum glacial-induced horizontal stresses (σ_h) would be dominantly oriented
487 parallel to the shelf break (Björn Lund personal communication; Lund et al., 2009). This is, dominantly
488 oriented N-S in the area of the Vestnesa Ridge (Fig. 1). Such stress orientation would not favour opening for
489 fluids along pre-existing NW-SE oriented faults associated with seepage activity at present (i.e., N-S oriented
490 faults would be the more vulnerable for opening). It is likely, though, that the repeated waxing and waning of the
491 ice sheet caused a cyclic modulation of the stress field (varying magnitude and orientation) and influenced the
492 dynamics of gas accumulations and favourably oriented faults along the Vestnesa Ridge in the past. Past glacial
493 stresses may provide then an alternative explanation for seepage along the entire Vestensa Ridge extent at given
494 periods of time (Fig. 6). This explanation is in line with the correlation between seepage and glacial-interglacial

495 events postulated for different continental margins e.g., for chimneys off the mid-Norwegian margin (Plaza-
496 Faverola et al., 2011), the Gulf of Lion (Riboulet et al., 2014), but also along the Vestnesa Ridge (Plaza-Faverola
497 et al., 2015; Schneider et al., 2018b).

498

499 A temporal variation in the stress field along the Vestnesa Ridge is also caused by its location on a constantly
500 growing plate. As the oceanic plate grows, the Vestnesa Ridge moves eastward with respect to the Molloy and
501 Knipovich Ridges, causing a westward shift in the regional stress field on the Vestnesa Ridge (Fig. 7). In future,
502 the eastern Vestnesa Ridge may temporarily move out of the tensile zone, while the western Vestnesa Ridge
503 moves into it (Fig. 7). This suggests that a negative effective stress and subsequent active seepage may reappear
504 at pockmarks to the west of the currently active seepage zone.

505

506 6.4 Implications for the understanding of near-surface deformation across passive margins

507

508 Our study is a first step in the investigation of the effect of regional stress on the dynamics of near-surface fluid
509 flow systems across passive margins. Analytical modelling of the spreading at the Molloy and the Knipovich
510 ridges shows that complex stress fields may arise from the interaction of the dynamics ~~at~~of plate boundaries and
511 exert an effect across passive margins. Although the Vestnesa Ridge is a unique case study due to its remarkable
512 proximity to the Arctic mid-ocean ridges, stresses generated by plate tectonic forces are expected to extend for
513 thousands of km (Fejerskov and Lindholm, 2000). Across a single passive margin a range of regional and local
514 factors may result in spatial stress field variations that can explain focusing of gas seepage at specific regions. For
515 instance, the pervasive seepage zone west of Prins Karl Fordland (PKF) on the west-Svalbard margin shelf break
516 (Fig. 1) could be under a stress regime where glacial rebound have had a more significant contribution to the total
517 stress field than it has had over the Vestnesa Ridge area. Wallmann et al., (2018) offered as explanation for
518 seepage at PKF that post glacial uplift lead to gas hydrate dissociation and associated seepage. Previously, several
519 other restudies argued for a gas-hydrate control on seepage in this region (e.g., Berndt et al., 2014; Portnov et al.,
520 2016; Westbrook et al., 2009). Since no gas hydrates have been found despite deep drilling (Riedel et al., 2018),
521 the influence of regional stresses provides an alternative and previously not contemplated explanation for seepage
522 in this area. The interactions between tectonic stress regimes and pore-fluid pressure we propose for explaining
523 seepage evolution along the Vestnesa Ridge may be applicable to seepage systems along other passive margins,
524 in particular along Atlantic passive margins where leakage from hydrocarbon reservoirs is prominent (e.g., the
525 mid-Norwegian margin, the Barents Sea, the North Sea, the north-east Greenland margin, the Mediterranean and

Formatted: Font: (Default) +Headings (Times New Roman),
11 pt

526 even the Scotia plate between Argentina and Antarctica) (e.g., Andreassen et al., 2017; Bünz et al., 2003; Hovland
527 and Sommerville, 1985; Riboulot et al., 2014; Somoza et al., 2014; Vis, 2017).

528

529 The intriguing, potential correlation between tectonic stress fields from mid-ocean ridge spreading and seepage
530 evolution along the Vestnesa Ridge, is an intriguing result that adds to the current debate about the quietness of
531 passive margins and the relation between deep crustal and near-surface deformation (Fejerskov and Lindholm,
532 2000; Fjeldskaar and Amantov, 2018; Lindholm et al., 2000; Olesen et al., 2013; Stein et al., 1989).

Formatted: English (United States)

533

534

535 **67- CONCLUSIONS**

536

537 Analytical modelling of the stress field generated by oblique spreading at the Molloy and Knipovich ridges in the
538 Fram Strait, suggests that tectonic forcing may be an important factor controlling faulting and seepage
539 distribution along the Vestnesa Ridge, off the west-Svalbard margin. Other important sources of stress such as
540 bathymetry and lithospheric bending, contributing to the actual state of stress off Svalbard, are not considered in
541 the modelling exercise presented here; thus, we cannot quantitatively assess whether ridge push has a dominant
542 effect on seepage activity. However, provided a certain degree of coupling between our analysis of how crustal
543 and near-surface deformation, it is plausible that stresses from plate spreading may affect the behaviour of
544 mapped Quaternary faults along the Vestnesa Ridge. Spreading at the Molloy and Knipovich ridges leads to a
545 spatial variation in the tectonic stress regime exerted along the Vestnesa Ridge, that may favour fluid migration
546 through pre-existing faults and fractures on the. The eastern Vestnesa Ridge is under a stress regime that is
547 favourable favours for fluid migration through pre-existing faults and fractures. on the eastern Vestnesa Ridge
548 where active seepage occurs. We suggest that pOur study supports a tectonic explanation for the observed
549 seepage pattern in the region. The resent day seepage is facilitated by opening of faults and fractures favourably
550 oriented with respect to principal stresses in a tensile stress regime or dilation on faults favourably oriented with
551 respect to principal stresses, facilitates the release of gas from zones of relatively high-pore fluid pressure at the
552 base of the gas hydrate stability zone. where pore fluid pressure overcomes the minimum horizontal stress.

553 Multiple seepage events along the entire extent of the Vestnesa Ridge, may have been induced by additional
554 sources of stress likely associated with glacial isostasy. Future reactivation of currently dormant pockmarks is
555 likely following the gradual westward propagation of the tensile stress zone on the Vestnesa Ridge as the
556 Eurasian plate drift towards the south-east. Despite the simplifying assumptions by the analytical model approach

557 implemented here, this study provides a first ~~order~~-assessment of how important understanding the state of stress
558 may be for reconstructing seepage activity in Arctic passive margins.

559

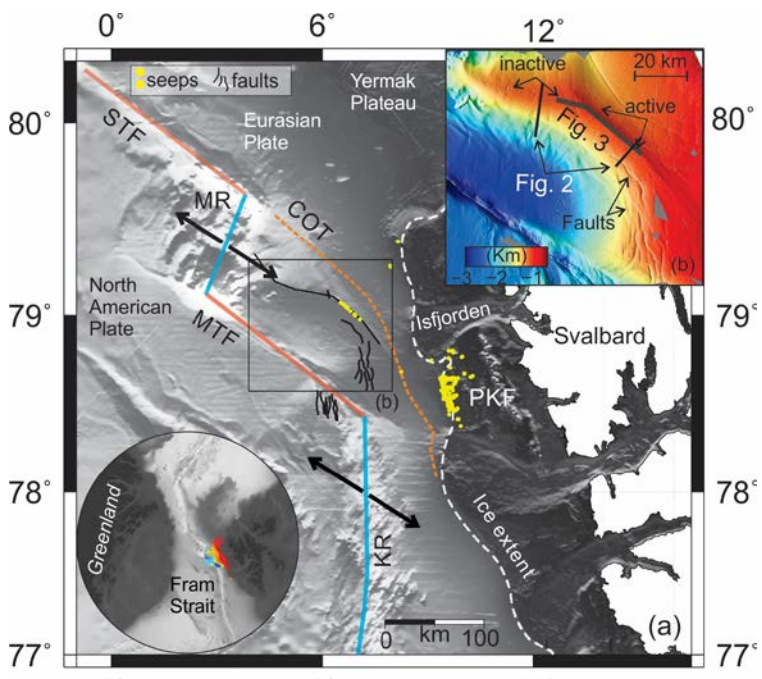
560 7- OUTLOOK

561 The effect of glacial stresses over the fluid flow system off west-Svalbard will be further tested (at least for the
562 Weichselian period) by implementing Lund et al., models using newly constrained Barents Sea ice-sheet models
563 (Patton et al., 2016). Additional sources of stress related to topography/bathymetry should be further investigated
564 as well to gain a comprehensive assessment of the effect of the total stress field on near-surface fluid migration in
565 the region.

566

567 Figures

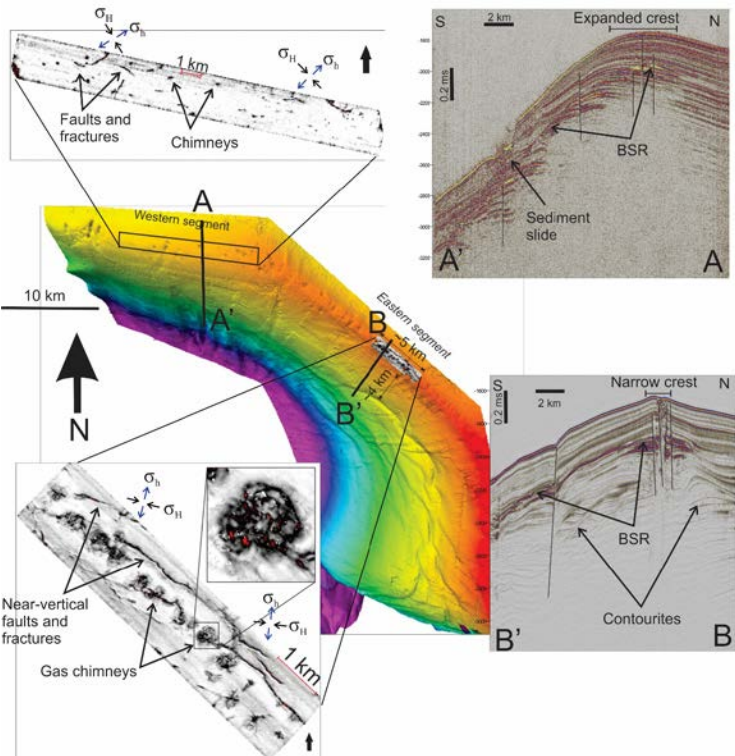
568



569

570 **Figure 1:** (a) International Bathymetry Chart of the Arctic Ocean (IBCAO) showing the geometry of mid-ocean
 571 ridges offshore the west-Svalbard margin; (b) High resolution bathymetry along the Vestnesa Ridge (UiT, R/V
 572 HH multi-beam system). Seafloor pockmarks are observed along the entire ridge but active seep sites are
 573 restricted to its eastern segment; PKF=Prins Karl Foreland; STF=Spitsbergen Transform Fault; MR=Molloy
 574 Ridge; MTF=Molloy Transform Fault; KR=Knipovich Ridge; COT=Continental-Oceanic Transition (Engen et
 575 al., 2008); Ice-Sheet Extent (Patton et al., 2016).

576



Formatted: Font: (Default) +Headings (Times New Roman),
 11 pt

577
 578 **Figure 2:** Composite figure with bathymetry and variance maps from 3D seismic data along the eastern and the
 579 western Vestnesa Ridge segments (modified from Plaza-Faverola et al., 2015). The orientation of maximum
 580 compressive horizontal stress (σ_h) and minimum horizontal stress (σ_b) predicted by the model are projected for

581 comparison with the orientation of fault segments. Notice favourable orientation for opening to fluids on the
582 eastern Vestnesa Ridge segment. Two-2D seismic transects (A-A' - Bünz et al., 2012 and B-B' – Johnson et al.,
583 2015) illustrate the morphological difference of the crest of the Vestnesa Ridge (i.e., narrow vs. extended)
584 believed to be determined by bottom current dominated deposition and erosion (Eiken and Hinz, 1993).

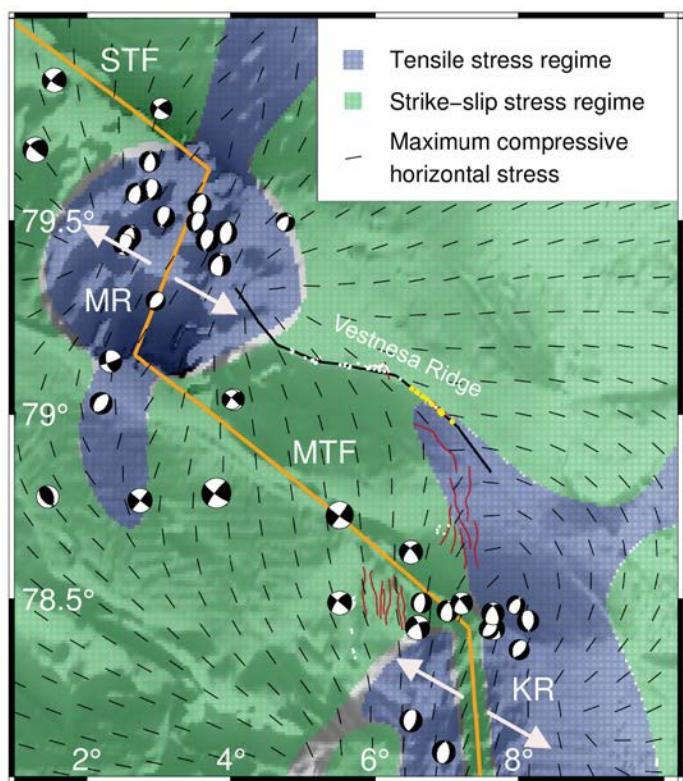
585 BSR=bottom simulating reflector.

586

587

588

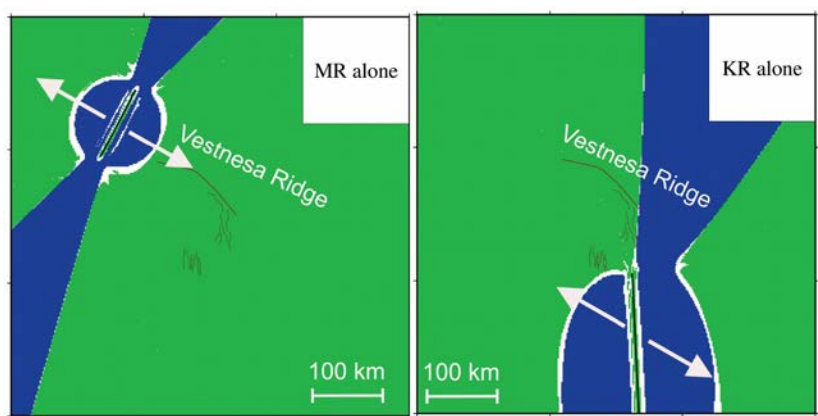
589



591

592 **Figure 3:** Modelled upper crustal tectonic stress field (blue – tensile and green - strike-slip regime) and stress
593 orientations, due to oblique spreading at Molloy Ridge (MR) and Knipovich Ridge (KR). The seismic line is
594 projected as reference for the crest of the Vestnesa Ridge. Red lines are faults, yellow dots seeps and white
595 circles inactive pockmarks. The focal mechanisms are from the ISC Online Bulletin (<http://www.isc.ac.uk>).

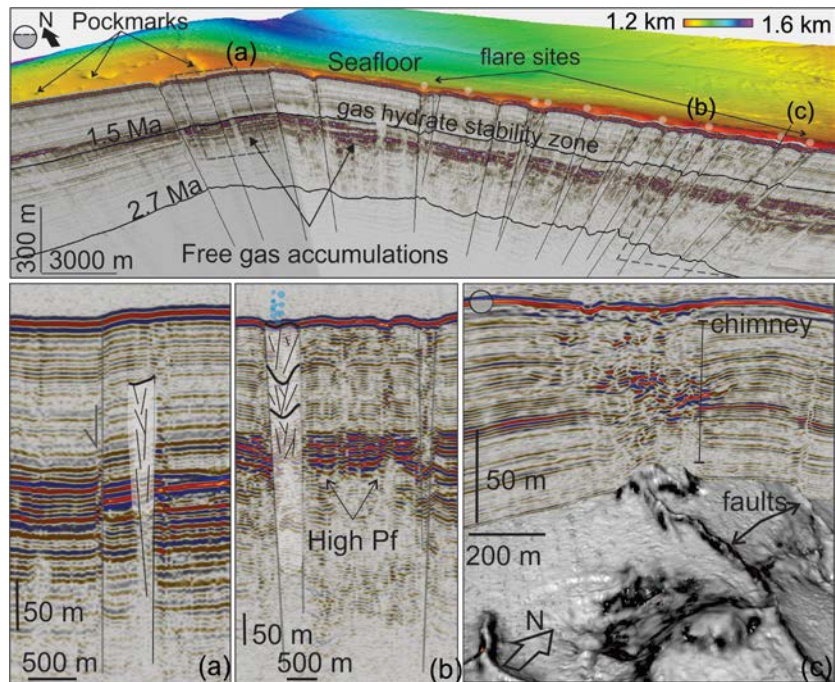
596



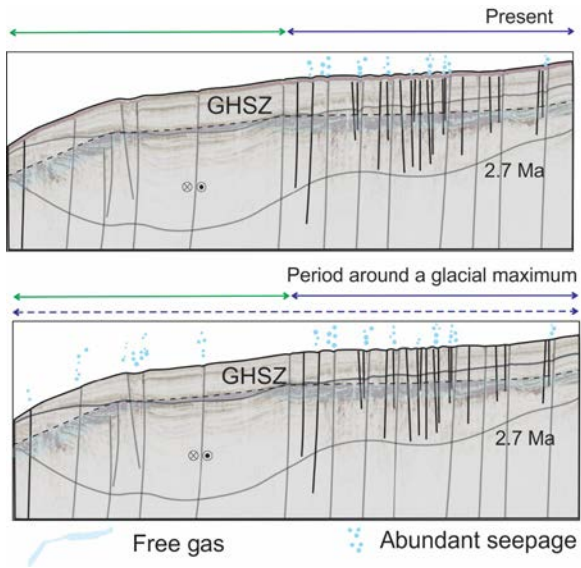
597

598 Figure 4: Stress field resulting from model runs with Molloy Ridge and Knipovich Ridge, respectively.

599

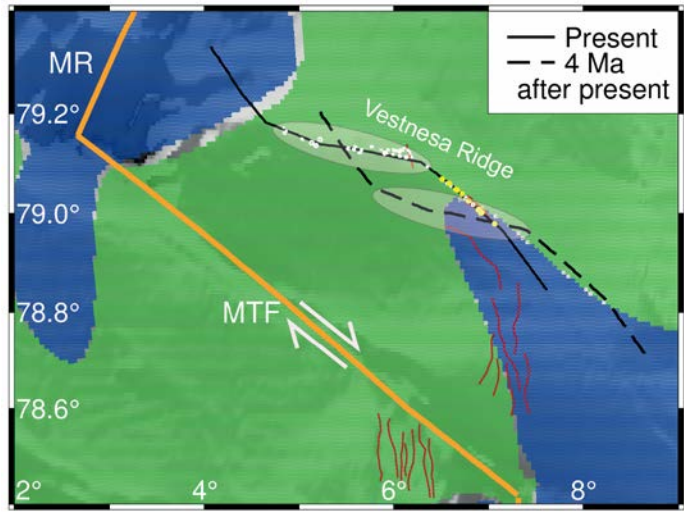


601 **Figure 5:** Integrated seismic and bathymetry image of the gas hydrate system along the Vestnesa Ridge. (a)
602 Outcropping N-S oriented fault located at the transition from the region where acoustic flares have been
603 documented to the region where no flares have been observed at pockmarks; (b) Gas chimneys with acoustic flare
604 associated and inferred high pore-fluid pressure (Pf) zone at the base of the gas hydrate stability zone; (c) Gas
605 chimney associated with faults and faults extending to near-surface strata. The same variance map in figure 2 is
606 projected at the depth where the map was extracted along a surface interpreted on the 3D seismic volume.
607



608

609 **Figure 6:** Conceptual model of the evolution of seepage coupled to faulting and spatial variations in the stress
 610 regime (tensile=blue; strike-slip=green) along the Vestnesa Ridge, offshore the west-Svalbard margin. At present
 611 day, tensile stress from mid-ocean ridge spreading (blue solid line) favours seepage exclusively on the eastern
 612 segment of the Vestnesa Ridge. Seepage on the western Vestnesa Ridge and other regions may have been
 613 induced repeatedly since the onset of glaciations 2.7 Ma ago (Mattingsdal et al., 2014), due to tensional flexural
 614 stresses in the isostatic forebulge around the time of glacial maximums.



615
616 **Figure 7:** Stress field in figure 3 showing the location of the Vestnesa Ridge at present and 4 Ma after present
617 time, assuming a constant spreading velocity of 7 mm/yr in the direction N125°E. The black polygon corresponds
618 to the seismic line in Plaza-Faverola et al., 2017 and partly shown in figure 3. It is presented as reference for the
619 crest of the eastern and western Vestnesa Ridge segments

620

621 **Appendix A**

622 **Model description**

623

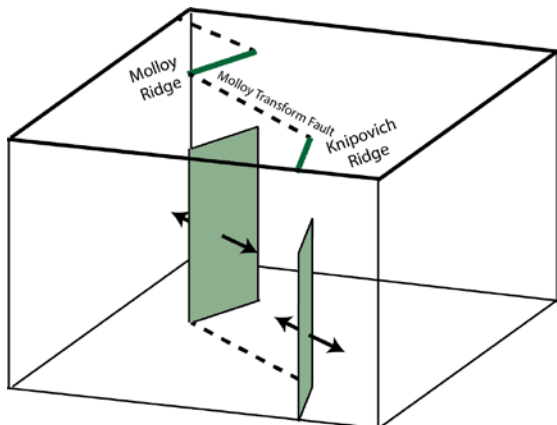
624 We use the analytical formulations of Okada (1985) for a finite rectangular dislocation source in elastic
625 homogeneous isotropic half-space (Fig. A.1). The dislocation source can be used to approximate deformation
626 along planar surfaces, such as volcanic dykes (e.g. Wright et al., 2006), sills (e.g. Pedersen and Sigmundsson,
627 2004), faults (e.g. Massonet et al., 1993) and spreading ridges (e.g. Keiding et al., 2009). More than one
628 dislocations can be combined to obtain more complex geometry of the source or varying deformation along a
629 planar source. The deformation of the source can be defined as either lateral shear (strike-slip for faults), vertical
630 shear (dip-slip at faults) or tensile opening.

631

632 The Okada model assumes flat Earth without inhomogeneities. While the flat-earth assumption is usually
633 adequate for regional studies (e.g. Wolf, 1984), the lateral inhomogeneities can sometimes cause considerable
634 effect on the deformation field (e.g. Okada, 1985). However, the dislocation model is useful as a first
635 approximation to the problem.

636

637 At mid-ocean ridges, deformation is driven by the continuous spreading caused primarily by gravitational stress
638 due to the elevation of the ridges, but also basal drag and possibly slab pull. Deformation occurs continuously in
639 the ductile part of the crust. Meanwhile, elastic strain builds in the upper, brittle part of the crust. To model this
640 setting, the upper boundary of the dislocation source must be located at the depth of the brittle-ductile transition
641 zone. The lower boundary of the source is set to some arbitrary large depth to avoid boundary effects.



642

643 **Fig A.1 Extract of model showing the location of the dislocation sources (light green) for Molloy and**
644 **Knipovich ridges. Note that the model is an infinite half-space, i.e. it has no lateral or lower boundary.**

645

646 The Okada model provides the displacements u_x , u_y , u_z (or velocities if deformation is time-dependent) at defined
647 grid points at the surface and subsurface. It also provides strain (or strain rates) defined as:

648

649 The stress field can then be calculated from the predicted strain rates. In homogeneous isotropic media, stress is
650 related to strain as:

651

652 where δ_{ij} is the Kronecker delta, λ is Lamé's first parameter, and μ is the shear modulus. Lamé's first parameter
653 does not have a physical meaning but is related to the shear modulus and Poisson's ratio (ν) as .
654 The absolute values of stress are in general difficult to model (e.g. Hergert and Heidbach, 2011), and not possible
655 with our analytical model. However, the model provides us with the orientations and relative magnitude of the
656 stresses. That is, we know the relative magnitudes of the vertical stress (σ_v), maximum horizontal stress (σ_H) and
657 minimum horizontal stress (σ_h). From this, the stress regime can be defined as either tensile ($\sigma_v > \sigma_H > \sigma_h$),
658 strike-slip ($\sigma_H > \sigma_v > \sigma_h$) or compressive ($\sigma_H > \sigma_h > \sigma_v$).

659

660 **Author contribution**

661 Andreia Plaza-Faverola conceived the paper idea. She is responsible for seismic data processing and
662 interpretation. Marie Keiding did the tectonic modelling. The paper is the result of integrated work between both.

663

664 **ACKNOWLEDGEMENTS**

665 This research is part of the Centre for Arctic Gas Hydrate, Environment and Climate (CAGE) supported by the
666 Research Council of Norway through its Centres of Excellence funding scheme grant No. 223259. Marie Keiding
667 is supported by the NEONOR2 project at the Geological Survey of Norway. Special thanks to Björn Lund, Peter
668 Schmidt, Henry Patton, and Alun Hubbard for their interest in the present project and constructive discussions
669 about isostasy and glacial stresses. We are thankful to various reviewers that have contributed to the
670 improvement of the manuscript. Seismic data is archived at CAGE – Centre for Arctic Gas Hydrate, Environment
671 and Climate, Tromsø, Norway and can be made available by contacting APF. Modelled stresses can be made
672 available by contacting MK.

673

674 **References:**

675 Ambrose, W. G., Panieri, G., Schneider, A., Plaza-Faverola, A., Carroll, M. L., Åström, E. K., Locke, W. L., and
676 Carroll, J.: Bivalve shell horizons in seafloor pockmarks of the last glacial-interglacial transition: a thousand years
677 of methane emissions in the Arctic Ocean, *Geochemistry, Geophysics, Geosystems*, 16, 4108-4129, 2015.
678 Andreassen, K., Hubbard, A., Winsborrow, M., Patton, H., Vadakkepuliyambatta, S., Plaza-Faverola, A.,
679 Gudlaugsson, E., Serov, P., Deryabin, A., and Mattingdal, R.: Massive blow-out craters formed by hydrate-
680 controlled methane expulsion from the Arctic seafloor, *Science*, 356, 948-953, 2017.
681 Árnadóttir, T., Lund, B., Jiang, W., Geirsson, H., Björnsson, H., Einarsson, P., and Sigurdsson, T.: Glacial rebound
682 and plate spreading: results from the first countrywide GPS observations in Iceland, *Geophysical Journal
683 International*, 177, 691-716, 2009.

684 Auriac, A., Whitehouse, P., Bentley, M., Patton, H., Lloyd, J., and Hubbard, A.: Glacial isostatic adjustment
685 associated with the Barents Sea ice sheet: a modelling inter-comparison, *Quaternary Science Reviews*, 147, 122-
686 135, 2016.

687 Berndt, C., Feseker, T., Treude, T., Krastel, S., Liebetrau, V., Niemann, H., Bertics, V. J., Dumke, I., Dünnbier, K.,
688 and Ferré, B.: Temporal constraints on hydrate-controlled methane seepage off Svalbard, *Science*, 343, 284-287,
689 2014.

690 Bünz, S., Mienert, J., and Berndt, C.: Geological controls on the Storegga gas-hydrate system of the mid-
691 Norwegian continental margin, *Earth and Planetary Science Letters*, 209, 291-307, 2003.

692 Bünz, S., Polyanov, S., Vadakkepuliyambatta, S., Consolaro, C., and Mienert, J.: Active gas venting through
693 hydrate-bearing sediments on the Vestnesa Ridge, offshore W-Svalbard, *Marine geology*, 2012.

694 Chand, S., Thorsnes, T., Rise, L., Brunstad, H., Stoddart, D., Bøe, R., Lågstad, P., and Svolsbru, T.: Multiple
695 episodes of fluid flow in the SW Barents Sea (Loppa High) evidenced by gas flares, pockmarks and gas hydrate
696 accumulation, *Earth and Planetary Science Letters*, 331, 305-314, 2012.

697 Consolaro, C., Rasmussen, T., Panieri, G., Mienert, J., Bünz, S., and Sztybor, K.: Carbon isotope (δ 13 C)
698 excursions suggest times of major methane release during the last 14 kyr in Fram Strait, the deep-water
699 gateway to the Arctic, *Climate of the Past*, 11, 669-685, 2015.

700 Crane, K., Sundvor, E., Buck, R., and Martinez, F.: Rifting in the northern Norwegian-Greenland Sea: Thermal
701 tests of asymmetric spreading, *Journal of Geophysical Research: Solid Earth*, 96, 14529-14550, 1991.

702 Crane, K., Doss, H., Vogt, P., Sundvor, E., Cherkashov, G., Poroshina, I., and Joseph, D.: The role of the
703 Spitsbergen shear zone in determining morphology, segmentation and evolution of the Knipovich Ridge, *Marine
704 geophysical researches*, 22, 153-205, 2001.

705 Crutchley, G. J., Berndt, C., Geiger, S., Klaeschen, D., Papenberg, C., Klaucke, I., Hornbach, M. J., Bangs, N. L., and
706 Maier, C.: Drivers of focused fluid flow and methane seepage at south Hydrate Ridge, offshore Oregon, USA,
707 *Geology*, 41, 551-554, 2013.

708 Davies, R. J., Mathias, S. A., Moss, J., Hustoft, S., and Newport, L.: Hydraulic fractures: How far can they go?,
709 *Marine and petroleum geology*, 37, 1-6, 2012.

710 DeMets, C., Gordon, R. G., and Argus, D. F.: Geologically current plate motions, *Geophysical Journal
711 International*, 181, 1-80, 2010.

712 DeVore, J. R., and Sawyer, D. E.: Shear strength of siliciclastic sediments from passive and active margins (0-100
713 m below seafloor): insights into seismic strengthening, in: *Submarine Mass Movements and their
714 Consequences*, Springer, 173-180, 2016.

715 Dickens, G. R.: Down the rabbit hole: Toward appropriate discussion of methane release from gas hydrate
716 systems during the Paleocene-Eocene thermal maximum and other past hyperthermal events, *Climate of the
717 Past*, 7, 831-846, 2011.

718 Dumke, I., Burwicz, E. B., Berndt, C., Klaeschen, D., Feseker, T., Geissler, W. H., and Sarkar, S.: Gas hydrate
719 distribution and hydrocarbon maturation north of the Knipovich Ridge, western Svalbard margin, *Journal of
720 Geophysical Research: Solid Earth*, 121, 1405-1424, 2016.

721 Ehlers, B.-M., and Jokat, W.: Subsidence and crustal roughness of ultra-slow spreading ridges in the northern
722 North Atlantic and the Arctic Ocean, *Geophysical Journal International*, 177, 451-462, 2009.

723 Eiken, O., and Hinz, K.: Contourites in the Fram Strait, *Sedimentary Geology*, 82, 15-32, 1993.

724 Eldholm, O., Faleide, J. I., and Myhre, A. M.: Continent-ocean transition at the western Barents Sea/Svalbard
725 continental margin, *Geology*, 15, 1118-1122, 1987.

726 Engen, Ø., Faleide, J. I., and Dyreng, T. K.: Opening of the Fram Strait gateway: A review of plate tectonic
727 constraints, *Tectonophysics*, 450, 51-69, 2008.

728 Faleide, J., Gudlaugsson, S., Eldholm, O., Myhre, A., and Jackson, H.: Deep seismic transects across the sheared
729 western Barents Sea-Svalbard continental margin, *Tectonophysics*, 189, 73-89, 1991.

730 Faleide, J. I., Solheim, A., Fiedler, A., Hjelstuen, B. O., Andersen, E. S., and Vanneste, K.: Late Cenozoic evolution
731 of the western Barents Sea-Svalbard continental margin, *Global and Planetary Change*, 12, 53-74, 1996.

732 Faulkner, D., Jackson, C., Lunn, R., Schlische, R., Shipton, Z., Wibberley, C., and Withjack, M.: A review of recent
733 developments concerning the structure, mechanics and fluid flow properties of fault zones, *Journal of Structural
734 Geology*, 32, 1557-1575, 2010.

735 Fejerskov, M., and Lindholm, C.: Crustal stress in and around Norway: an evaluation of stress-generating
736 mechanisms, *Geological Society, London, Special Publications*, 167, 451-467, 2000.

737 Fjeldskaar, W., and Amantov, A.: Effects of glaciations on sedimentary basins, *Journal of Geodynamics*, 118, 66-
738 81, 2018.

739 Franek, P., Plaza-Faverola, A., Mienert, J., Buentz, S., Ferré, B., and Hubbard, A.: Microseismicity linked to gas
740 migration and leakage on the Western Svalbard Shelf, *Geochemistry, Geophysics, Geosystems*, 18, 4623-4645,
741 2017.

742 Gaina, C., Nikishin, A., and Petrov, E.: Ultraslow spreading, ridge relocation and compressional events in the East
743 Arctic region: A link to the Eurekan orogeny?, *arktos*, 1, 16, 2015.

744 Geersen, J., Scholz, F., Linke, P., Schmidt, M., Lange, D., Behrmann, J. H., Völker, D., and Hensen, C.: Fault zone
745 controlled seafloor methane seepage in the rupture area of the 2010 Maule Earthquake, Central Chile,
746 *Geochemistry, Geophysics, Geosystems*, 17, 4802-4813, 2016.

747 Grauls, D., and Baleix, J.: Role of overpressures and in situ stresses in fault-controlled hydrocarbon migration: A
748 case study, *Marine and Petroleum Geology*, 11, 734-742, 1994.

749 Grunnaleite, I., Fjeldskaar, W., Wilson, J., Faleide, J., and Zweigert, J.: Effect of local variations of vertical and
750 horizontal stresses on the Cenozoic structuring of the mid-Norwegian shelf, *Tectonophysics*, 470, 267-283,
751 2009.

752 Gölke, M., and Coblenz, D.: Origins of the European regional stress field, *Tectonophysics*, 266, 11-24, 1996.

753 Heidbach, O., Rajabi, M., Reiter, K., and Ziegler, M.: World stress map 2016, *Science*, 277, 1956-1962, 2016.

754 Hillis, R. R.: Coupled changes in pore pressure and stress in oil fields and sedimentary basins, *Petroleum
755 Geoscience*, 7, 419-425, 2001.

756 Hong, W. L., Sauer, S., Panieri, G., Ambrose, W. G., James, R. H., Plaza-Faverola, A., and Schneider, A.: Removal
757 of methane through hydrological, microbial, and geochemical processes in the shallow sediments of pockmarks
758 along eastern Vestnesa Ridge (Svalbard), *Limnology and Oceanography*, 61, 2016.

759 Hovland, M., and Sommerville, J. H.: Characteristics of two natural gas seepages in the North Sea, *Marine and
760 Petroleum Geology*, 2, 319-326, 1985.

761 Hovland, M.: On the self-sealing nature of marine seeps, *Continental Shelf Research*, 22, 2387-2394, 2002.

762 Hunter, S., Goldobin, D., Haywood, A., Ridgwell, A., and Rees, J.: Sensitivity of the global submarine hydrate
763 inventory to scenarios of future climate change, *Earth and Planetary Science Letters*, 367, 105-115, 2013.

764 Hustoft, S., Bünz, S., and Mienert, J.: Three-dimensional seismic analysis of the morphology and spatial
765 distribution of chimneys beneath the Nyegga pockmark field, offshore mid-Norway, *Basin Research*, 22, 465-
766 480, 2010.

767 Hustoft, S., Bunz, S., Mienert, J., Chand, S.: Gas hydrate reservoir and active methane-venting province in
768 sediments on < 20 Ma young oceanic crust in the Fram Strait, offshore NW-Svalbard, *Earth and Planetary*
769 *Science Letters*, 284, 12-24, 10.1016/j.epsl.2009.03.038, 2009.

770 Jakobsson, M., Backman, J., Rudels, B., Nylander, J., Frank, M., Mayer, L., Jokat, W., Sangiorgi, F., O'Regan, M.,
771 and Brinkhuis, H.: The early Miocene onset of a ventilated circulation regime in the Arctic Ocean, *Nature*, 447,
772 986-990, 2007.

773 Jansen, E., Sjøholm, J., Bleil, U., and Erichsen, J.: Neogene and Pleistocene glaciations in the northern
774 hemisphere and late Miocene—Pliocene global ice volume fluctuations: Evidence from the Norwegian Sea, in:
775 *Geological History of the Polar Oceans: Arctic versus Antarctic*, Springer, 677-705, 1990.

776 Jansen, E., and Sjøholm, J.: Reconstruction of glaciation over the past 6 Myr from ice-borne deposits in the
777 Norwegian Sea, *Nature*, 349, 600, 1991.

778 Johnson, J. E., Mienert, J., Plaza-Faverola, A., Vadakkepuliyambatta, S., Knies, J., Bünz, S., Andreassen, K., and
779 Ferré, B.: Abiotic methane from ultraslow-spreading ridges can charge Arctic gas hydrates, *Geology*, G36440.
780 36441, 2015.

781 Jokat, W., Lehmann, P., Damaske, D., and Nelson, J. B.: Magnetic signature of North-East Greenland, the Morris
782 Jesup Rise, the Yermak Plateau, the central Fram Strait: constraints for the rift/drift history between Greenland
783 and Svalbard since the Eocene, *Tectonophysics*, 691, 98-109, 2016.

784 Judd, A., and Hovland, M.: Seabed fluid flow: the impact on geology, biology and the marine environment,
785 Cambridge University Press, 2009.

786 Jung, N.-H., Han, W. S., Watson, Z., Graham, J. P., and Kim, K.-Y.: Fault-controlled CO₂ leakage from natural
787 reservoirs in the Colorado Plateau, East-Central Utah, *Earth and Planetary Science Letters*, 403, 358-367, 2014.

788 Karstens, J., and Berndt, C.: Seismic chimneys in the Southern Viking Graben—Implications for palaeo fluid
789 migration and overpressure evolution, *Earth and Planetary Science Letters*, 412, 88-100, 2015.

790 Karstens, J., Hafliðason, H., Becker, L. W., Berndt, C., Rüpke, L., Planke, S., Liebetrau, V., Schmidt, M., and
791 Mienert, J.: Glacigenic sedimentation pulses triggered post-glacial gas hydrate dissociation, *Nature*
792 *communications*, 9, 635, 2018.

793 Keiding, M., Lund, B., and Árnadóttir, T.: Earthquakes, stress, and strain along an obliquely divergent plate
794 boundary: Reykjanes Peninsula, southwest Iceland, *Journal of Geophysical Research: Solid Earth*, 114, 2009.

795 Knies, J., Matthiessen, J., Vogt, C., Laberg, J. S., Hjelstuen, B. O., Smelror, M., Larsen, E., Andreassen, K., Eidvin,
796 T., and Vorren, T. O.: The Plio-Pleistocene glaciation of the Barents Sea—Svalbard region: a new model based on
797 revised chronostratigraphy, *Quaternary Science Reviews*, 28, 812-829,
798 <http://dx.doi.org/10.1016/j.quascirev.2008.12.002>, 2009.

799 Knies, J., Daszynska, M., Plaza-Faverola, A., Chand, S., Sylta, Ø., Bünz, S., Johnson, J. E., Mattingdal, R., and
800 Mienert, J.: Modelling persistent methane seepage offshore western Svalbard since early Pleistocene, *Marine*
801 *and Petroleum Geology*, 91, 800-811, 2018.

802 Lindholm, C. D., Bungum, H., Hicks, E., and Villagran, M.: Crustal stress and tectonics in Norwegian regions
803 determined from earthquake focal mechanisms, *Geological Society, London, Special Publications*, 167, 429-439,
804 2000.

805 Lund, B., and Townend, J.: Calculating horizontal stress orientations with full or partial knowledge of the
806 tectonic stress tensor, *Geophysical Journal International*, 170, 1328-1335, 2007.

807 Lund, B., Schmidt, P., and Hieronymus, C.: Stress evolution and fault stability during the Weichselian glacial
808 cycle, *Swedish Nuclear Fuel and Waste Management Co, Stockholm, Sweden, Tech. Rep. TR-09-15*, 2009.

809 Lund, B., and Schmidt, P.: Stress evolution and fault stability at Olkiluoto during the Weichselian glaciation,
810 Report for Posiva Oy, 2011.

811 Mattingdal, R., Knies, J., Andreassen, K., Fabian, K., Husum, K., Grøsfjeld, K., and De Schepper, S.: A new 6 Myr
812 stratigraphic framework for the Atlantic–Arctic Gateway, *Quaternary Science Reviews*, 92, 170-178, 2014.

813 Minshull, T., and White, R.: Sediment compaction and fluid migration in the Makran accretionary prism, *Journal*
814 *of Geophysical Research: Solid Earth*, 94, 7387-7402, 1989.

815 Moore, J. C., and Vrolijk, P.: Fluids in accretionary prisms, *Reviews of Geophysics*, 30, 113-135, 1992.

816 Morgan, W. J.: 13. Hotspot tracks and the opening of the Atlantic and Indian Oceans, *The oceanic lithosphere*, 7,
817 443, 1981.

818 Myhre, A. M., and Eldholm, O.: The western Svalbard margin (74–80 N), *Marine and Petroleum Geology*, 5, 134-
819 156, 1988.

820 Naliboff, J., Lithgow-Bertelloni, C., Ruff, L., and de Koker, N.: The effects of lithospheric thickness and density
821 structure on Earth's stress field, *Geophysical Journal International*, 188, 1-17, 2012.

822 Nasuti, A., and Olesen, O.: Chapter 4: Magnetic data. In: Hopper J.R., Funck T., Stoker T., Arting U., Peron-
823 Pinvidic G., Doornbehal H. & Gaina C. (eds) *Tectonostratigraphic Atlas of the North-East Atlantic Region*.

824 Geological Survey of Denmark and Greenland (GEUS), Copenhagen, Denmark, 41–51. , 2014.

825 Okada, Y.: Surface deformation due to shear and tensile faults in a half-space, *Bulletin of the seismological*
826 *society of America*, 75, 1135-1154, 1985.

827 Olesen, O., Bungum, H., Dehls, J., Lindholm, C., Pascal, C., and Roberts, D.: Neotectonics, seismicity and
828 contemporary stress field in Norway—mechanisms and implications, *Quaternary Geology of Norway*, Geological
829 Survey of Norway Special Publication, 13, 145-174, 2013.

830 Panieri, G., Bünz, S., Fornari, D. J., Escartin, J., Serov, P., Jansson, P., Torres, M. E., Johnson, J. E., Hong, W., and
831 Sauer, S.: An integrated view of the methane system in the pockmarks at Vestnesa Ridge, 79° N, *Marine*
832 *Geology*, 390, 282-300, 2017.

833 Patton, H., Hubbard, A., Andreassen, K., Winsborrow, M., and Stroeven, A. P.: The build-up, configuration, and
834 dynamical sensitivity of the Eurasian ice-sheet complex to Late Weichselian climatic and oceanic forcing,
835 *Quaternary Science Reviews*, 153, 97-121, 2016.

836 Petersen, C. J., Bünz, S., Hustoft, S., Mienert, J., and Klaeschen, D.: High-resolution P-Cable 3D seismic imaging
837 of gas chimney structures in gas hydrated sediments of an Arctic sediment drift, *Marine and Petroleum*
838 *Geology*, doi: 10.1016/j.marpetgeo.2010.06.006, 1-14, DOI: 10.1016/j.marpetgeo.2010.06.006, 2010.

839 Planke, S., Eriksen, F. N., Berndt, C., Mienert, J., and Masson, D.: P-Cable high-resolution seismic, *Oceanography*,
840 22, 85, 2009.

841 Plaza-Faverola, A., Bünz, S., and Mienert, J.: Repeated fluid expulsion through sub-seabed chimneys offshore
842 Norway in response to glacial cycles, *Earth and Planetary Science Letters*, 305, 297-308,
843 10.1016/j.epsl.2011.03.001, 2011.

844 Plaza-Faverola, A., Bünz, S., Johnson, J. E., Chand, S., Knies, J., Mienert, J., and Franek, P.: Role of tectonic stress
845 in seepage evolution along the gas hydrate-charged Vestnesa Ridge, *Fram Strait*, *Geophys. Res. Lett.*, 42, 733-
846 742, 2015.

847 Plaza-Faverola, A., Henrys, S., Pecher, I., Wallace, L., and Klaeschen, D.: Splay fault branching from the Hikurangi
848 subduction shear zone: Implications for slow slip and fluid flow, *Geochemistry, Geophysics, Geosystems*, 17,
849 5009-5023, 2016.

850 Plaza-Faverola, A., Vadakkepuliyambatta, S., Hong, W. L., Mienert, J., Bünz, S., Chand, S., and Greinert, J.:
851 Bottom-simulating reflector dynamics at Arctic thermogenic gas provinces: an example from Vestnesa Ridge,
852 offshore west-Svalbard, *Journal of Geophysical Research: Solid Earth*, 2017.

853 Portnov, A., Vadakkepuliyambatta, S., Mienert, J., and Hubbard, A.: Ice-sheet-driven methane storage and
854 release in the Arctic, *Nature communications*, 7, 10314, 2016.

855 Riboulot, V., Thomas, Y., Berné, S., Jouet, G., and Cattaneo, A.: Control of Quaternary sea-level changes on gas
856 seeps, *Geophys. Res. Lett.*, 41, 4970-4977, 2014.

857 Riedel, M., Wallmann, K., Berndt, C., Pape, T., Freudenthal, T., Bergenthal, M., Bünz, S., and Bohrmann, G.: In
858 situ temperature measurements at the Svalbard Continental Margin: Implications for gas hydrate dynamics,
859 *Geochemistry, Geophysics, Geosystems*, 19, 1165-1177, 2018.

860 Roy, S., Senger, K., Braathen, A., Noormets, R., Hovland, M., and Olaussen, S.: Fluid migration pathways to
861 seafloor seepage in inner Isfjorden and Adventfjorden, Svalbard, Geological controls on fluid flow and seepage
862 in western Svalbard fjords, Norway. An integrated marine acoustic study, 2014.

863 Salomatin, A., and Yusupov, V.: Acoustic investigations of gas “flares” in the Sea of Okhotsk, *Oceanology*, 51,
864 857, 2011.

865 Salomon, E., Koehn, D., Passchier, C., Hackspacher, P. C., and Glasmacher, U. A.: Contrasting stress fields on
866 correlating margins of the South Atlantic, *Gondwana research*, 28, 1152-1167, 2015.

867 Schiffer, C., Tegner, C., Schaeffer, A. J., Pease, V., and Nielsen, S. B.: High Arctic geopotential stress field and
868 implications for geodynamic evolution, *Geological Society, London, Special Publications*, 460, 441-465, 2018.

869 Schneider, A., Panieri, G., Lepland, A., Consolaro, C., Crémère, A., Forwick, M., Johnson, J., Plaza-Faverola, A.,
870 Sauer, S., and Knies, J.: Methane seepage at Vestnesa Ridge (NW Svalbard) since the Last Glacial Maximum,
871 *Quaternary Science Reviews*, 193, 98-117, 2018a.

872 Schneider, A., Panieri, G., Lepland, A., Consolaro, C., Crémère, A., Forwick, M., Johnson, J. E., Plaza-Faverola, A.,
873 Sauer, S., and Knies, J.: Methane seepage at Vestnesa Ridge (NW Svalbard) since the Last Glacial Maximum,
874 *Quaternary Science Reviews*, 193, 98-117, <https://doi.org/10.1016/j.quascirev.2018.06.006>, 2018b.

875 Sibson, R. H.: Crustal stress, faulting and fluid flow, *Geological Society, London, Special Publications*, 78, 69-84,
876 1994.

877 Skarke, A., Ruppel, C., Kodis, M., Brothers, D., and Lobecker, E.: Widespread methane leakage from the sea floor
878 on the northern US Atlantic margin, *Nature Geoscience*, 7, 657-661, 2014.

879 Smith, A. J., Mienert, J., Bünz, S., and Greinert, J.: Thermogenic methane injection via bubble transport into the
880 upper Arctic Ocean from the hydrate-charged Vestnesa Ridge, Svalbard, *Geochemistry, Geophysics,
881 Geosystems*, 2014.

882 Somoza, L., León, R., Medialdea, T., Pérez, L. F., González, F. J., and Maldonado, A.: Seafloor mounds, craters
883 and depressions linked to seismic chimneys breaching fossilized diagenetic bottom simulating reflectors in the
884 central and southern Scotia Sea, Antarctica, *Global and Planetary Change*, 123, 359-373, 2014.

885 Steffen, H., Kaufmann, G., and Wu, P.: Three-dimensional finite-element modeling of the glacial isostatic
886 adjustment in Fennoscandia, *Earth and Planetary Science Letters*, 250, 358-375, 2006.

887 Stein, S., Cloetingh, S., Sleep, N. H., and Wortel, R.: Passive margin earthquakes, stresses and rheology, in:
888 *Earthquakes at North-Atlantic Passive Margins: Neotectonics and Postglacial Rebound*, Springer, 231-259, 1989.

889 Svensen, H., Planke, S., Malthe-Sørensen, A., Jamtveit, B., Myklebust, R., Eidem, T. R., and Rey, S. S.: Release of
890 methane from a volcanic basin as a mechanism for initial Eocene global warming, *Nature*, 429, 542-545, 2004.

891 Sztybor, K., and Rasmussen, T. L.: Late glacial and deglacial palaeoceanographic changes at Vestnesa Ridge,
892 Fram Strait: Methane seep versus non-seep environments, *Palaeogeography, Palaeoclimatology, Palaeoecology*,
893 476, 77-89, 2017.

894 Turcotte, D., Ahern, J., and Bird, J.: The state of stress at continental margins, *Tectonophysics*, 42, 1-28, 1977.

895 Turcotte, D. L., and Schubert, G.: *Geodynamics*, Cambridge University Press, New York, 2002.

896 Urlaub, M., Talling, P. J., Zervos, A., and Masson, D.: What causes large submarine landslides on low gradient (<
897 2°) continental slopes with slow (~ 0.15 m/kyr) sediment accumulation?, *Journal of Geophysical Research: Solid
898 Earth*, 120, 6722-6739, 2015.

899 Vanneste, M., Guidard, S., and Mienert, J.: Arctic gas hydrate provinces along the western Svalbard continental
900 margin, *Norwegian Petroleum Society Special Publications*, 12, 271-284, 2005.

901 Vis, G.-J.: Geology and seepage in the NE Atlantic region, *Geological Society, London, Special Publications*, 447,
902 SP447. 416, 2017.

903 Vogt, P. R., Crane, K., Sundvor, E., Max, M. D., and Pfirman, S. L.: Methane-generated (?) pockmarks on young,
904 thickly sedimented oceanic crust in the Arctic: Vestnesa ridge, Fram strait, *Geology*, 22, 255-258, 1994.

905 Waghorn, K. A., Bünz, S., Plaza-Faverola, A., and Johnson, J. E.: 3D Seismic Investigation of a Gas Hydrate and
906 Fluid Flow System on an Active Mid-Ocean Ridge; Svyatogor Ridge, Fram Strait, *Geochemistry, Geophysics,
907 Geosystems*, 2018.

908 Wallmann, K., Riedel, M., Hong, W., Patton, H., Hubbard, A., Pape, T., Hsu, C., Schmidt, C., Johnson, J., and
909 Torres, M.: Gas hydrate dissociation off Svalbard induced by isostatic rebound rather than global warming,
910 *Nature communications*, 9, 83, 2018.

911 Westbrook, G. K., Thatcher, K. E., Rohling, E. J., Piotrowski, A. M., Palike, H., Osborne, A. H., Nisbet, E. G.,
912 Minshull, T. A., Lanoiselle, M., James, R. H., Huhnerbach, V., Green, D., Fisher, R. E., Crocker, A. J., Chabert, A.,
913 Bolton, C., Beszczynska-Möller, A., Berndt, C., and Aquilina, A.: Escape of methane gas from the seabed along
914 the West Spitsbergen continental margin, *Geophys. Res. Lett.*, 36, 5, L1560810.1029/2009gl039191, 2009.

915 Zoback, M. D., and Zoback, M. L.: 34 State of stress in the Earth's lithosphere, *International Geophysics*, 81, 559-
916 XII, 2002.

917